Interaction Notes

Note 435

December 1983

Interaction of High-Altitude Electromagnetic Pulse (HEMP) with Transmission and Distribution Lines: An Early-Time Consideration*

K.S.H. Lee
F.C. Yang
N. Engheta

Abstract

In the first few tens of nanoseconds after an HEMP strikes the transmission and distribution lines of an electric power system, the induced transients on these lines rise to very high values. During these early times one cannot in general apply transmission line theory to calculate the transients. In this report a linear, time-domain scattering theory is employed to calculate such transients induced on a multi-conductor line above a finitely conducting ground. The relative importance of various inducing effects is discussed, which include the incident field, the fields scattered by neighboring conductors, and the field reflected from the ground. The effect of the conductor's resistivity is found to be negligible on the induced transients, whereas the incident field has the most dominant inducing effect. A formulation of the HEMP-induced corona on a wire is given with some introductory remarks.

The linear, time-domain scattering theory is applied to a typical 3ϕ, 765 kV transmission line and a 3ϕ, 13.2 kV distribution line. In the first 20 nanoseconds or so, the conductors of the transmission line can have induced currents of a few kiloamperes and the normal electric fields in the order of one-half megavolts per meter on the phase conductors and a few tens of megavolts per meter on the shield conductors. On the distribution line the induced currents are less by a factor of 5 to 6 but the electric fields are 5 to 6 times greater than those on the phase conductors of the transmission line.

---

*This work was prepared for the Zaininger Engineering Company under subcontract to the Oak Ridge National Laboratory for the Division of Electric Energy Systems of the Department of Energy.

CONTENTS

Section		Page
	PREFACE	3
I.	INTRODUCTION	4
II.	FORMULATION	7
III.	A SINGLE WIRE IN FREE SPACE	12
IV.	EFFECT OF NEIGHBORING WIRES	19
V.	EFFECT OF GROUND REFLECTED FIELD	25
VI.	EFFECT OF WIRE RESISTIVITY	31
VII.	THE COMBINED EFFECT	34
VIII.	APPLICATIONS	37
	REFERENCES	53
	APPENDIX: EFFECT OF CORONA	54

PREFACE

The authors would like to thank the following individuals for helpful discussions: P.R. Barnes and B.W. McConnell of ORNL; H. Neff of the University of Tennessee; H.W. Zaininger of ZECO; Rene Aguero of Dikewood.

I. INTRODUCTION

The high-altitude electromagnetic pulse (HEMP) generated from a nuclear detonation beyond 50 km above the earth surface is known to have a fast rise and a large amplitude (Fig. 1). It can cover a large ground area, such as the continent of the United States, with a peak electric field in the order of 40 - 80 kV/m. When a large network of conductors (e.g., a power grid) is exposed to such a field, large and fast transients can be induced on the network.

Although the interaction of HEMP with above-ground power lines has been studied quite extensively in the past (see, for example, Refs. 1 and 2), there are few important features that have heretofore been neglected. First, past studies are invariably based on the transmission line theory, which is applicable to low frequencies and late times, typically for times greater than tens of microseconds. Second, above-ground power lines are systems of multiconductors and, hence, the mutual interaction among the conductors must be taken into account. Third, since the HEMP field rises very quickly to a large amplitude, the induced electric field on the conductors may exceed, in the first few tens of nanoseconds, the breakdown field of the surrounding air, thereby causing such nonlinear phenomena as corona and flashover to occur. Therefore, an accurate early-time calculation is necessary before entering into the nonlinear region. The present study deals with the early-time interaction of HEMP with multiconductor lines above ground.

The approach to be adopted is a linear, time-domain scattering theory which is discussed in Section II. Section III treats the interaction of HEMP with a single wire in free space. The important result is a successful derivation of an accurate, simple, analytical expression for the

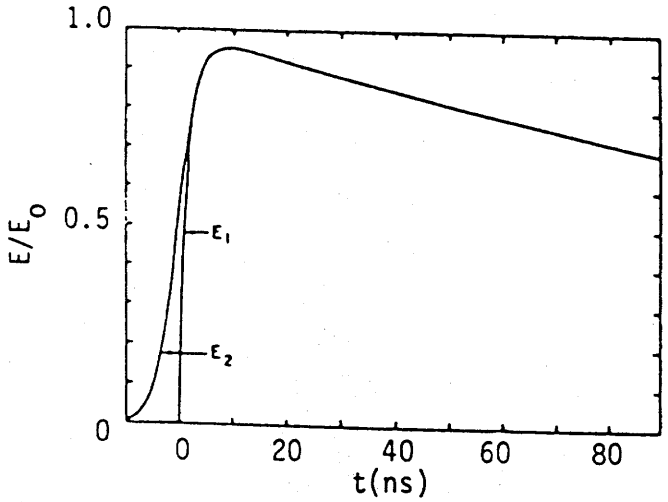

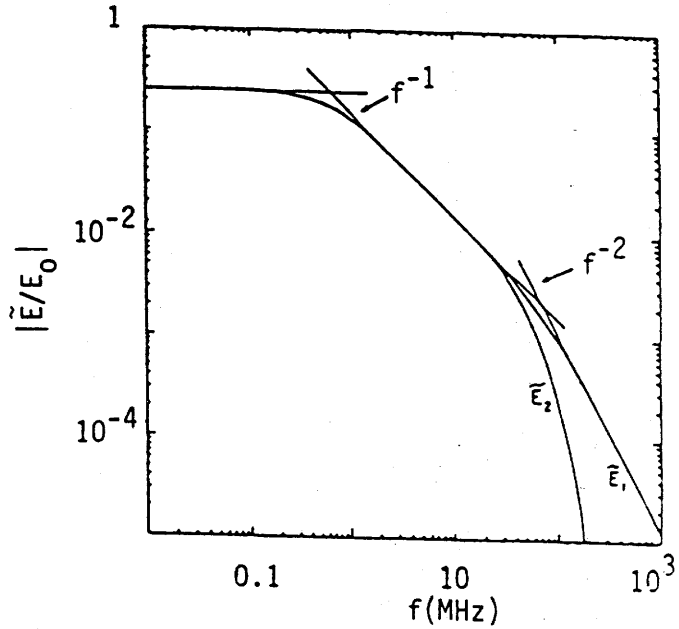

$$E_1 = E_0(e^{-\alpha t} - e^{-\beta t})u(t) \ , \quad E_2 = E_0(e^{\alpha t} + e^{-\beta t}) - 1$$

$$\alpha = 4 \times 10^6 \ \text{sec}^{-1} \ , \quad \beta = 4.78 \times 10^8 \ \text{sec}^{-1}$$

Figure 1. Two typical HEMP waveforms and their spectra.

induced current, which provides the basic ideas for the subsequent sections. The effects of neighboring wires, ground reflected field, and the wire resistivity are calculated in Sections IV - VI. The combined effect is shown in Section VII, where the time variations of the total induced current and radial electric field are given for a two-conductor line above ground. Section VII is devoted to two example calculations: a typical 3ϕ 765 kV single-circuit transmission line, and a typical 3ϕ 13.2 kV single-circuit distribution line. Some introductory remarks on the effect of corona are relegated to an appendix.

II. FORMULATION

Figure 2 is the geometry of the problem, which shows a set of parallel conductors or wires above a finitely conducting ground and immersed in an EMP plane-wave field. The quantities to be calculated are the current and radial electric field induced on each wire.

The relatively simpler problem of a single overhead line above ground has engaged the interest of many investigators [3-6]. An exact treatment of this problem for the entire frequency spectrum or time regime is very difficult mainly due to the presence of a conducting ground. Hence, for reason of tractability one looks at the problem in different time (or frequency) regimes and employs a different technique in each regime, as depicted in Figure 3. For times greater than the diffusion time (T_3) in the ground corresponding to a skin depth of approximately three times the height of the wire above the ground, one may use the restrictive transmission-line theory in which the ground is approximated by a simple, although frequency-dependent, inductance and resistance term. For earlier times (i.e., for $T_3 > t > T_2$) or higher frequencies one may use the transmission-line theory of Carson or King and Wu [3, 4]. For times less than T_2 there is no simplified theory except the full-blown Maxwell's equations with appropriate boundary and initial conditions. The full-blown theory is labeled as the scattering theory in Figure 3 which applies from $t = 0$ when the EMP hits the point of observation on any of the conductors to $t = \infty$ when everything has subsided.

For very early times (i.e., for $t < T_1$) before the ground reflected wave hits the wire, the wire responds to the incident wave alone. Subsequently, the incident wave upon reflection from the ground comes into play. Next, the scattered wave of the wire upon reflection from the ground also enters into

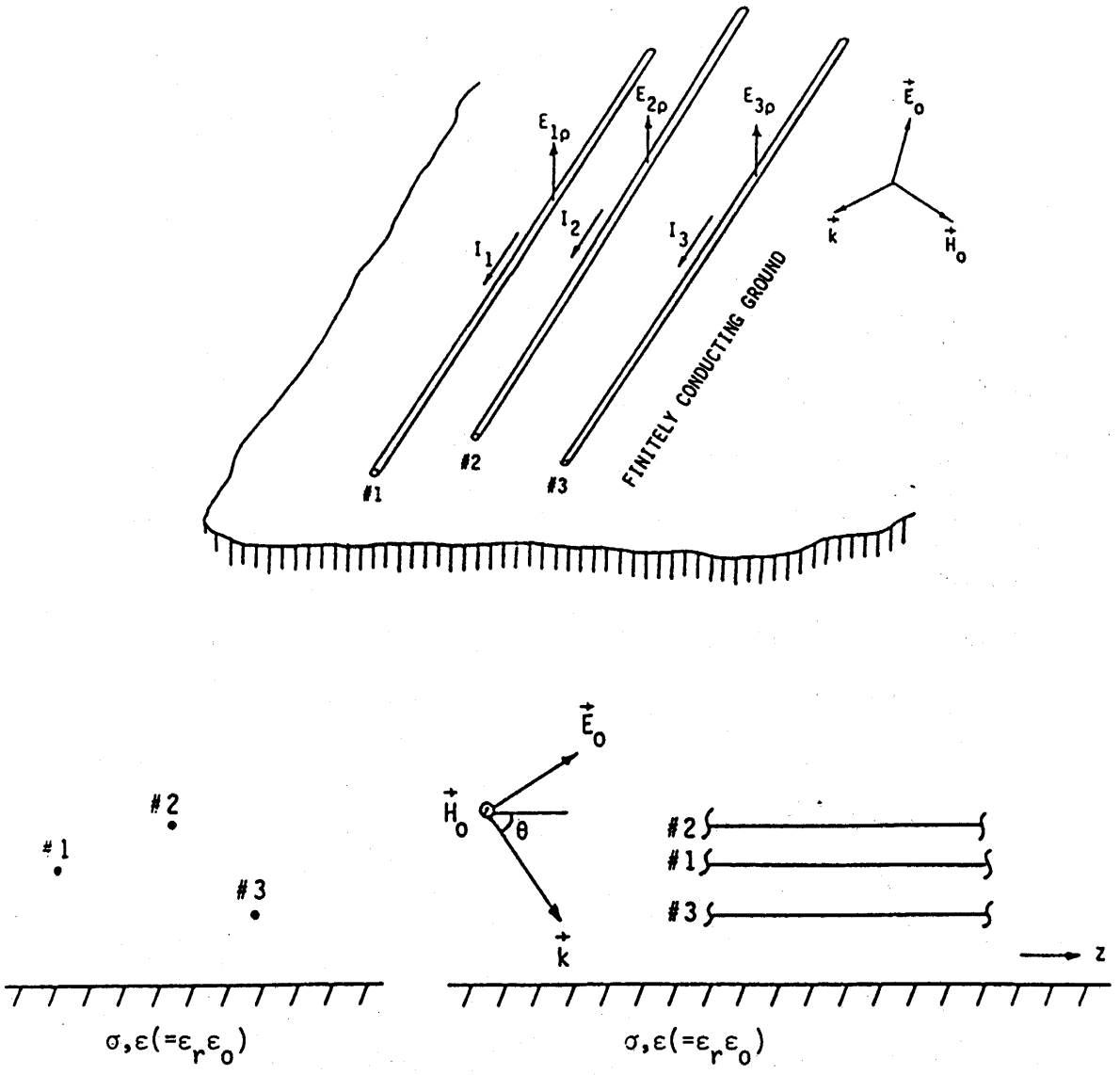

Figure 2. An example of three parallel wires above a finitely conducting ground.

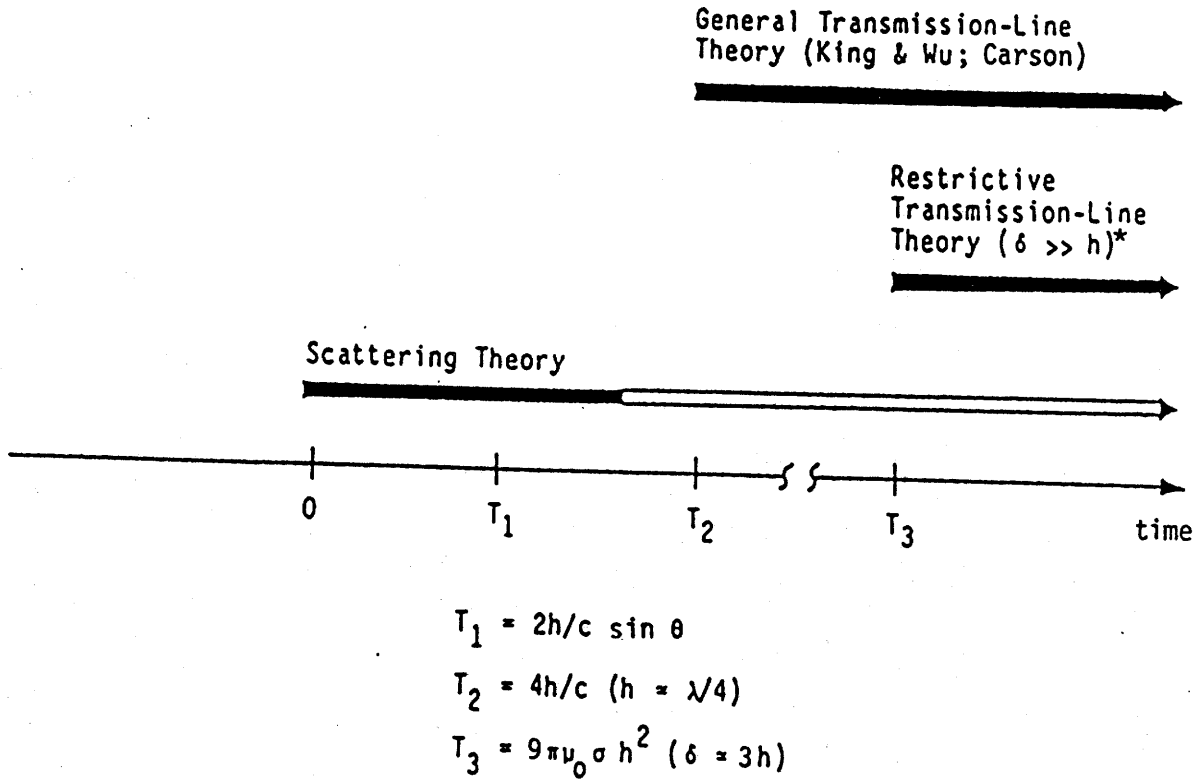

Figure 3. Different techniques for different time regimes for an overhead line. The height of the line from ground is h, and the ground conductivity is σ.

* This approach is adopted in Transmission Line Reference Book, 345 kV and Above, EPRI, 1982 [7].

the picture. As time goes on, more and more terms contribute to the total induced current and charge on the wire. Carrying out the above idea for the geometry in Figure 2 one can write down for, say, the induced current on wire #1,

$$I_1(t) = I_{11}(t)u(t - t_1) + I_{12}(t)u(t - t_2) + I_{13}(t)u(t - t_3) + I_{1g}(t)u(t - t_g) + ... \quad (1)$$

where I_{11} = current induced on wire #1 by the incident field alone; $I_{12}(I_{13})$ = current induced on wire #1 by the scattered field from wire #2 (#3); I_{1g} = current induced on wire #1 by the ground reflected field. Furthermore, the time delays in Equation 1 are defined as follows:

$t_1 = (z/c) \cos \theta - (a_1/c) \sin \theta$

= time delay due to oblique incidence and wire thickness with radius a_1

$t_2 = (z/c) \cos \theta - [(a_1 + a_2)/c] \sin \theta + [(h_1 - h_2)/c] \sin \theta + (d_{12}/c) \sin \theta$

= time delay due to separation of wire #2 from wire #1, where d_{12} is the separation, a_i and h_i are the radius and height of wire #i.

t_3 = same as t_2 with wire #3 replacing wire #2

$t_g = (z/c) \cos \theta - (a_1/c) \sin \theta + (2h_1/c) \sin \theta$

= time delay due to height of wire #1 from ground.

Once I_1 is known, the induced radial field $E_{1\rho}$ on the surface of wire #1 can be obtained from the continuity equation. Thus,

$$E_{1\rho} = \frac{Z_o I_1}{2\pi a_1} \cos \theta \quad (2)$$

For wire #2 one simply interchanges the subscripts 1 and 2 in the above

equations.

Equations 1 and 2 are the starting point for the calculations to follow. The calculations will include terms up to the first scattering, i.e., those terms explicitly shown in Equation 1.

III. A SINGLE WIRE IN FREE SPACE

Consider the I_{11} term in Equation 1, the current induced on wire #1 by the incident EMP alone. For the time being, let the incident wave be an impulse, i.e.,

$$\vec{E}_\delta = \vec{E}_0 \delta\ (t - \hat{k}\cdot\vec{r}/c)$$

where $\hat{k}$ is the unit vector in the direction of wave propagation. The current I_δ induced by this impulsive wave is given by [8]

$$I_\delta = \frac{2\pi c E_0}{Z_0 \sin\theta} \cdot \frac{1}{2\pi j} \int \frac{e^{s\tau} ds}{sK_0[(sa/c)\sin\theta]}, \qquad \tau = t - (z/c)\cos\theta$$

$$= \frac{2\pi c E_0}{Z_0 \sin\theta} \int_0^\infty \frac{I_0(x) e^{-x[c\tau/(a\sin\theta)]}}{x[K_0^2(x) + \pi^2 I_0^2(x)]}\, dx \qquad (3)$$

where θ is defined in Figure 2, and I_0 and K_0 are the modified Bessel function of the zeroth order of the first and second kind, a is the radius of the wire, Z_0 and c are the free-space impedance and speed of light. Making use of the fact that a/c < 0.1 nanoseconds or so, one can approximate Equation 3 by

$$I_\delta \simeq \frac{E_0}{L} u(t^*), \qquad t^* = \tau + (a/c)\sin\theta$$

$$L = \frac{Z_0}{2\pi c} \sin\theta\ \ell n\ (\frac{2ct^*}{\Gamma a \sin\theta}) \qquad (4)$$

with u being the unit step function and Γ = exponential of Euler's constant = 1.7810....

If the incident wave has the form

$$\vec{E}_{inc} = \vec{E}_0 f(t - \hat{k}\cdot\vec{r}/c)$$

then

$$I(\tau) = \int_{-\infty}^{\tau} I_{\delta}(t')f(\tau - t')dt'$$

$$= E_0 \int_{-\infty}^{\tau} \frac{u[t' + (a/c)\sin\theta]}{L[t' + (a/c)\sin\theta]} f(\tau - t')dt'$$

$$= E_0 \int_{0}^{\infty} \frac{u(t^* - t")}{L(t^* - t")} f(t")dt"$$

$$\simeq \frac{E_0}{L(t^*)} \int_{0}^{t^*} f(t")dt" \qquad (5)$$

The last step follows from the fact that L is a slowly varying function of time. For $f = \exp(-\alpha t) - \exp(-\beta t)$, Equation 5 gives

$$I = \frac{E_0}{L}\left[\frac{1}{\alpha}(1 - e^{-\alpha t^*}) - \frac{1}{\beta}(1 - e^{-\beta t^*})\right] \qquad (6)$$

This approximate expression is compared in Figure 4 to the highly accurate result reported in Reference 6, and the agreement is excellent.

Figures 5 and 6 give the time history of I_{11}, while Figure 7 shows the radial electric field for specific values of E_0, α and β, as shown in the figure captions. It can be concluded that the induced current I_{11} can rise up to tens of kiloamperes in a few hundred nanoseconds, whereas the induced radial electric field (or voltage gradient) can reach the critical field, which is taken to be 15 kV/cm, in a few nanoseconds. In Figure 8 is plotted the time t_c as a function of the wire radius a at the moment when the induced radial field E_ρ on the wire surface reaches the critical field E_c.

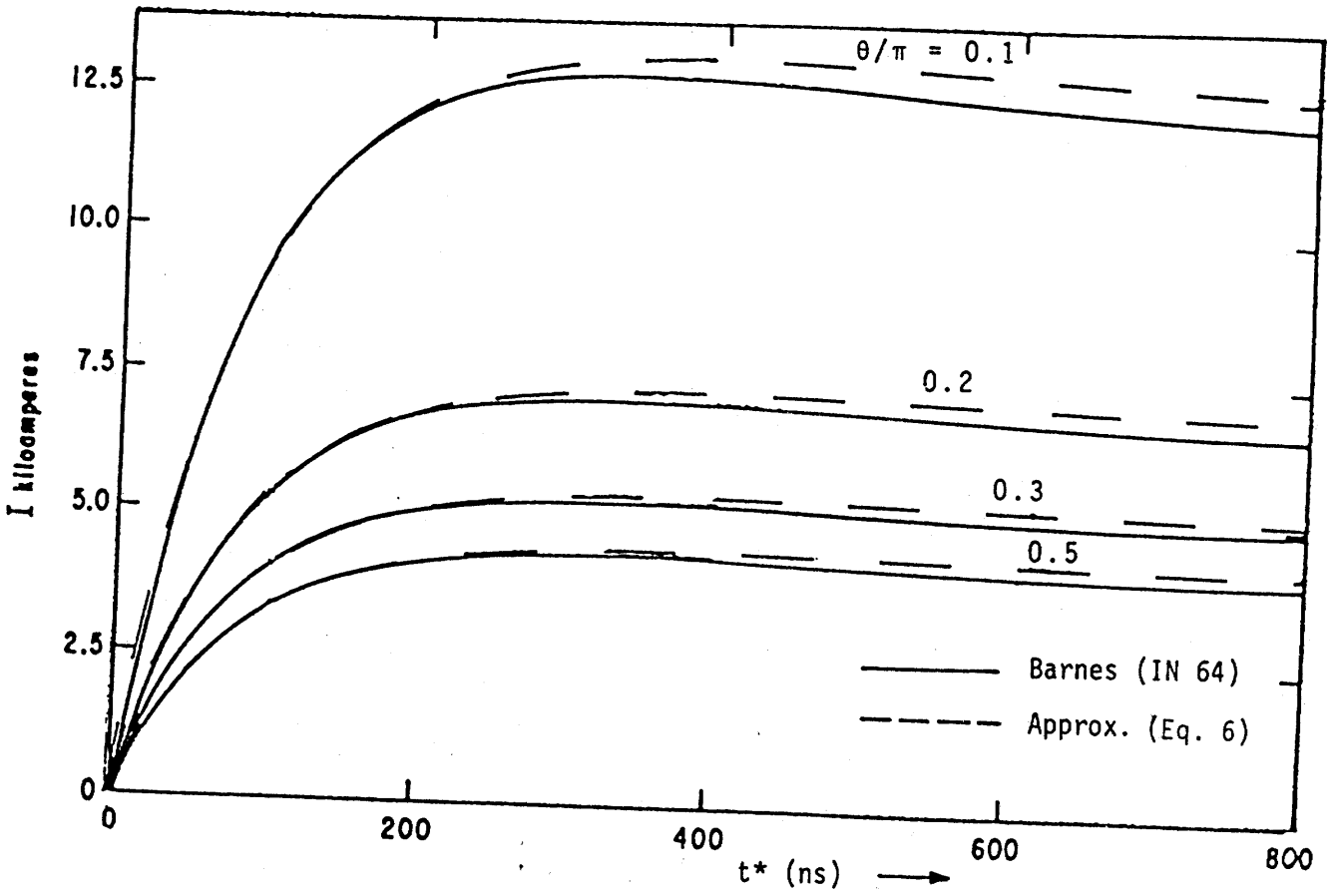

Figure 4. Comparison of the approximate repression 6 and the accurate numerical results (IN 64) for $E_o = 10^5$ kV/m, $\alpha = 10^7$ sec^{-1}, $\beta = 5 \times 10^8$ sec^{-1}, and and a = 0.3 cm.

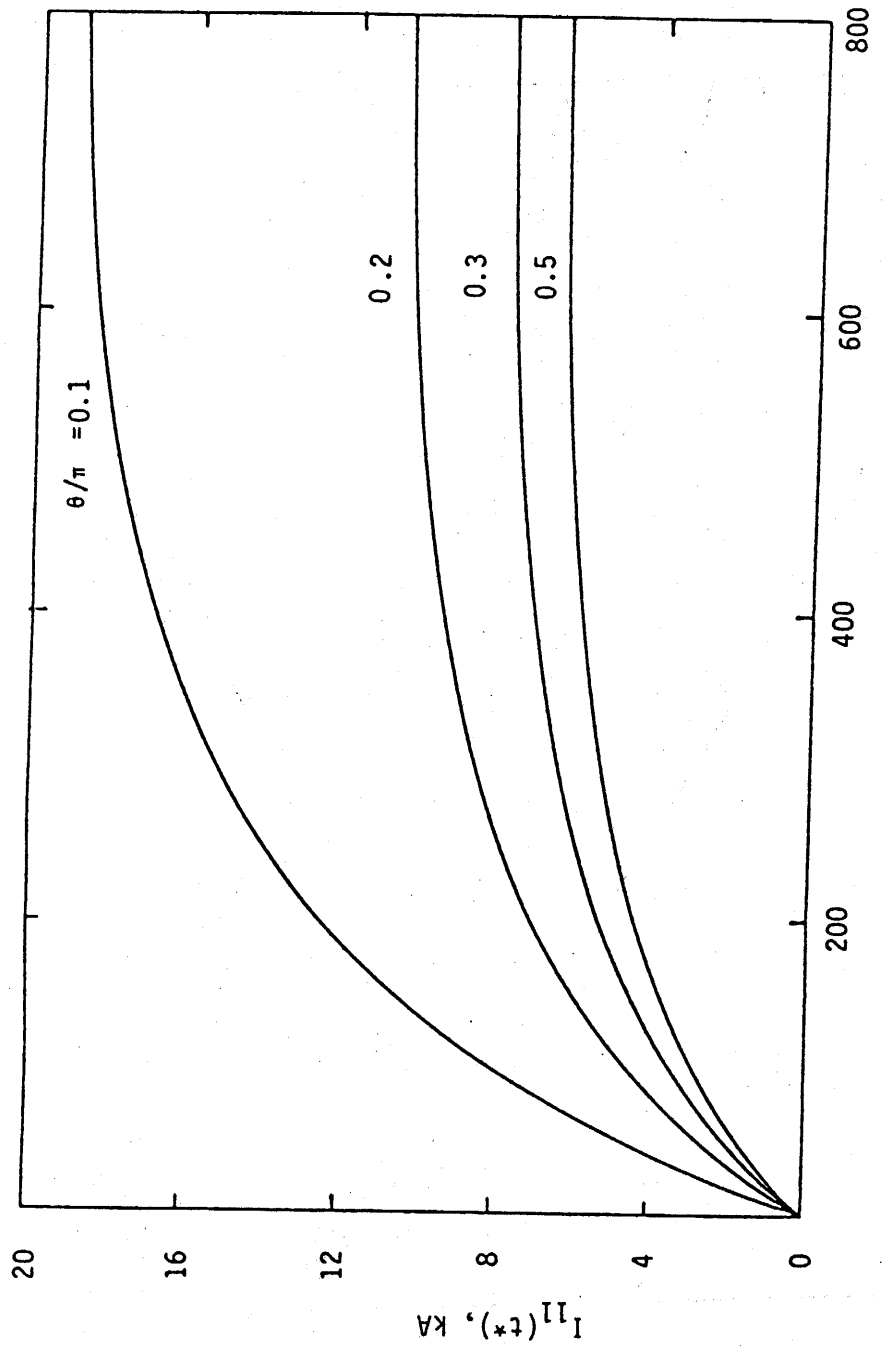

Figure 5. Induced current I_{11} for incident EMP with E_o = 52.5 kV/m, $\alpha = 4.0 \times 10^6$ sec^{-1}, $\beta = 4.78 \times 10^8$ sec^{-1}; and a = 2 cm.

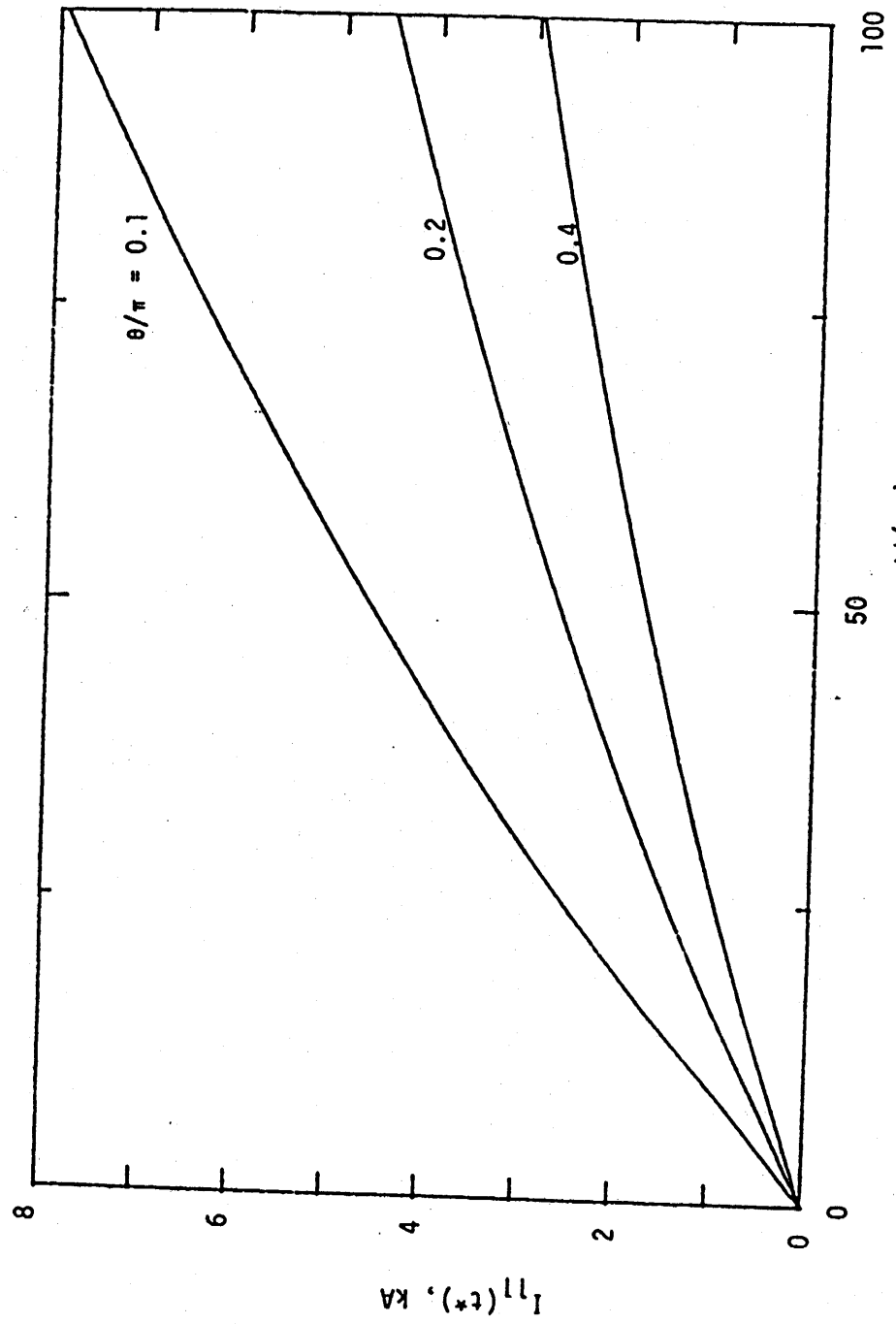

Figure 6. Current induced by incident EMP with E_0 = 52.5 kV/m, $\alpha = 4.0 \times 10^6$ sec^{-1}, $\beta = 4.78 \times 10^8$ sec^{-1}; a = 2 cm.

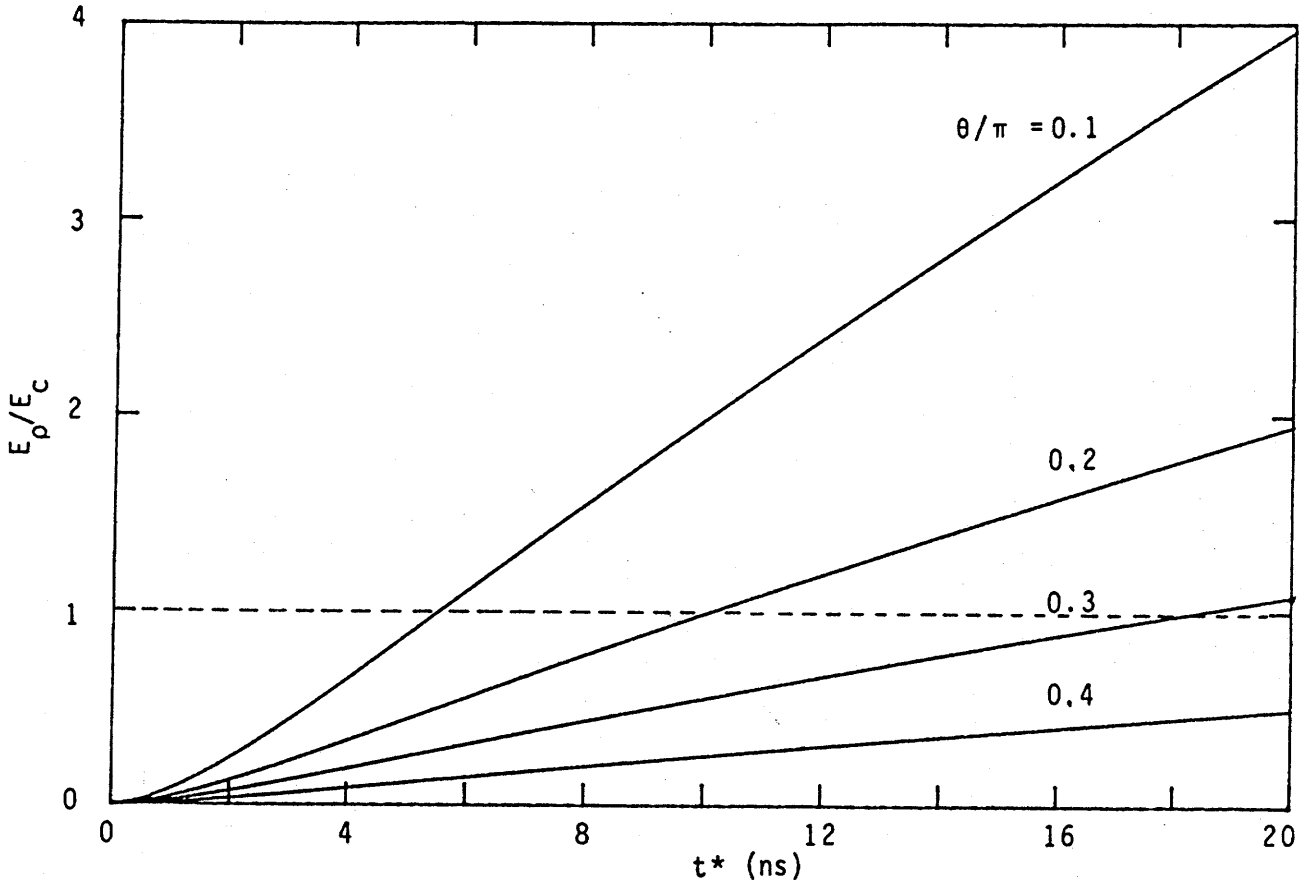

Figure 7. Normalized radial electric field induced by incident EMP with E_o = 52.5 kV/m, α = 4.0 X 10^6 sec^{-1}, β = 4.78 X 10^8 sec^{-1}; E_c = 15 kV/cm; and a = 2 cm.

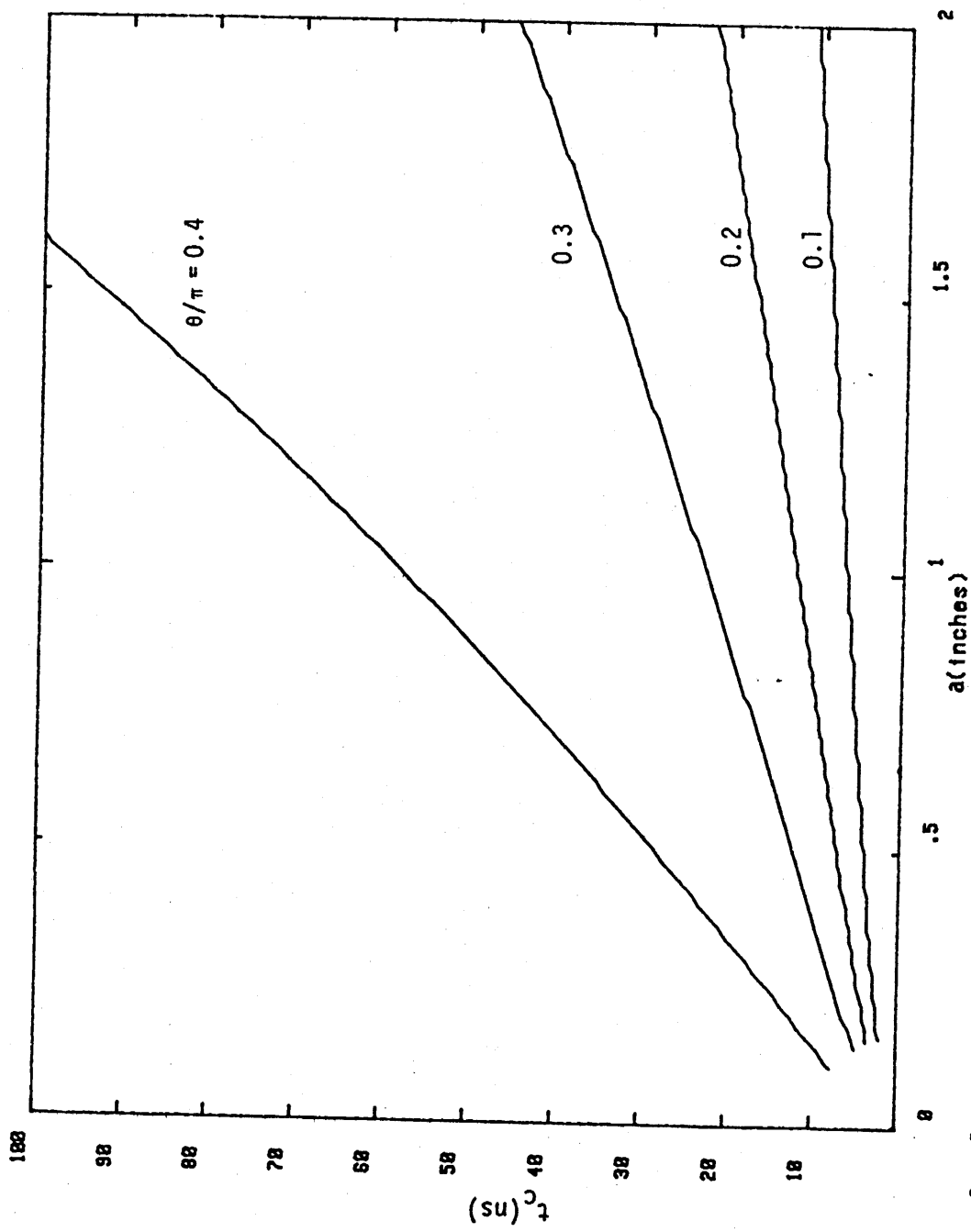

Figure 8. Dependence on the wire radius a of the time t_c when E_ρ reaches E_c (15kV/cm).

IV. EFFECT OF NEIGHBORING WIRES

Consider now the term I_{12} in Equation 1, the current on wire #1 induced by the scattered field from wire #2 alone.

The scattered field $\tilde{E}_{12}$ from wire #2 and evaluated along wire #1 is given by

$$\tilde{E}_{12} = -E_o\tilde{F} \sin\theta \frac{H_o^{(2)}(kd \sin\theta)}{H_o^{(2)}(ka_2 \sin\theta)} e^{jk(h_2 - h_1)\sin\theta} e^{-jkz\cos\theta} \qquad (7)$$

where $\tilde{F}$ is the Fourier transform of the incident waveform f(t), d is the separation of the wires, h_1 and h_2 are the heights of wire #1 and #2 from the ground, a_2 is the radius of wire #2, and $H_o^{(2)}$ is the Hankel function of zeroth order of the second kind. The current $\tilde{I}_{12}$ induced by the field given by Equation 7 is

$$\tilde{I}_{12} = \frac{4\tilde{E}_{12}}{Z_o \sin\theta} \frac{1}{k \sin\theta H_o^{(2)}(ka_1 \sin\theta)} \qquad (8)$$

where a_1 is the radius of wire #1. Converting Equation 8 to the Laplace domain with s replacing $j\omega$ and taking the inverse Laplace transform of the resulting expression, one gets

$$I_{12} = {}^{-1}\left\{\frac{1}{K_o[(s/c)a_1 \sin\theta]}\right\} \otimes L^{-1}\left\{K_o[(s/c)d \sin\theta]\, e^{-(s/c)z\cos\theta} \cdot e^{(s/c)(h_2 - h_1)\sin\theta}\right\} \otimes L^{-1}\left\{\frac{-2\pi cE_o\tilde{F}}{Z_o \sin\theta} \cdot \frac{1}{K_o[(s/c)a_2 \sin\theta]}\right\} \qquad (9)$$

where $\otimes$ denotes the convolution integral, and L^{-1} the inverse Laplace transform operator. The second expression in Equation 9 can be evaluated in

the same manner that leads one from Equation 3 to Equation 4. Thus, one gets the following approximate expression for I_{12}:

$$I_{12} \simeq -E_o \frac{M_{12}}{L_1 L_2} \int_0^{t^*} f(t)dt \tag{10}$$

where $t^* = t - t_2$, t_2 having been defined before, and

$$L_1 = \frac{Z_o}{2\pi c} \sin\theta \, \ell n\left(\frac{2ct^*}{\Gamma a_1 \sin\theta}\right), \quad L_2 = \frac{Z_o}{2\pi c} \sin\theta \, \ell n\left(\frac{2ct^*}{\Gamma a_2 \sin\theta}\right)$$

$$M_{12} = \frac{Z_o}{2\pi c} \sin\theta \cosh^{-1}\left(\frac{ct^*}{d \sin\theta} + 1\right) \tag{11}$$

Equation 10 is plotted in Figure 9 in which $a_1 = a_2 = 2$ cm, d = 9 m and the incident field is the same as that given in Figure 5. Note that the scattered field from wire #2 will induce a current on wire #1, which diminishes the current induced by the incident field alone. Figures 10 through 12 show the current and radial electric field induced by the incident and the scattered field. The effect of a neighboring wire on the induced current and radial electric field can be readily obtained by comparing these figures with the corresponding Figures 5 through 7.

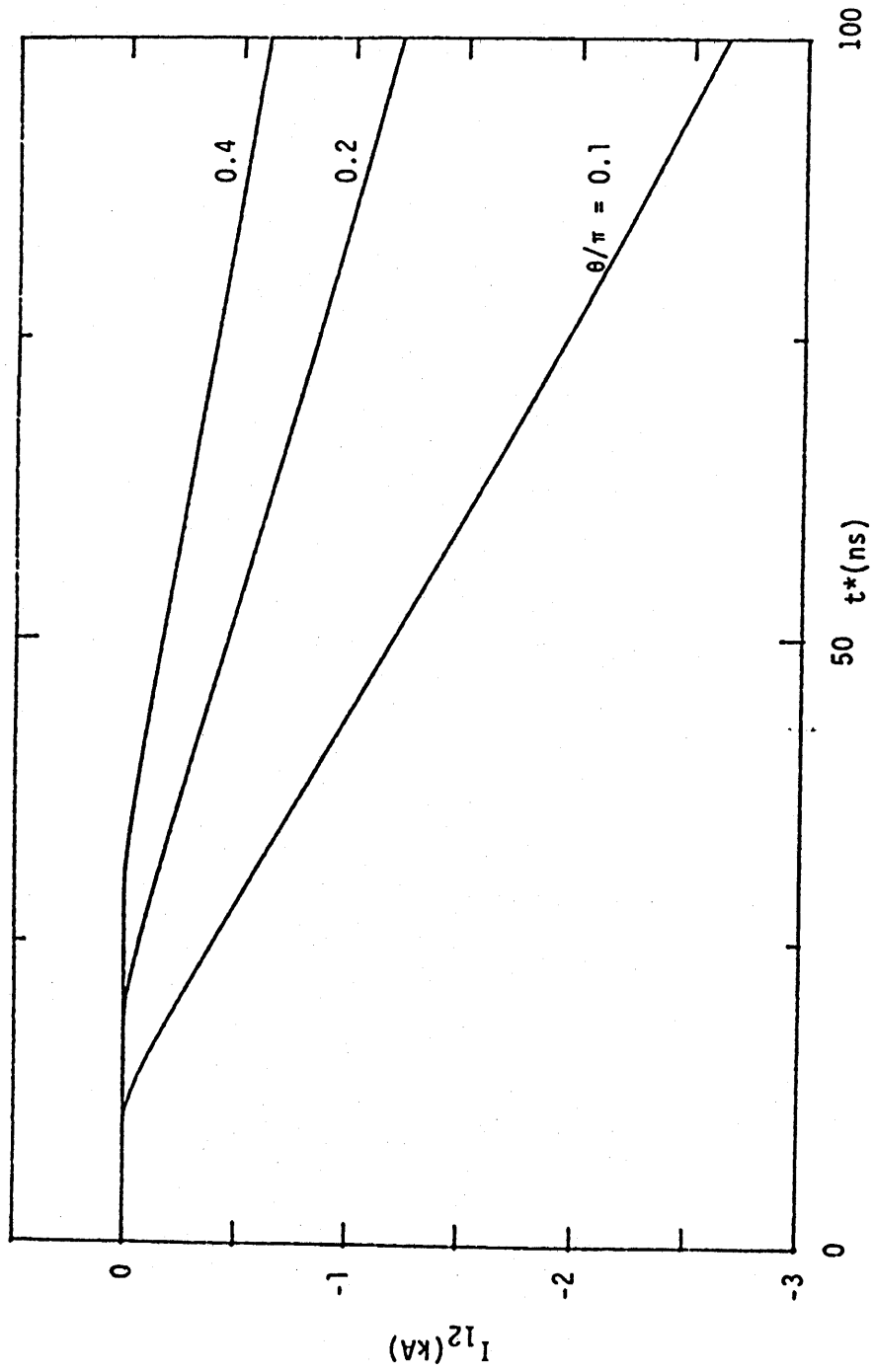

Figure 9. Induced current on conductor #1 by the scattered field from conductor #2. Both conductors are at the same height from the ground and separated by 9 m.

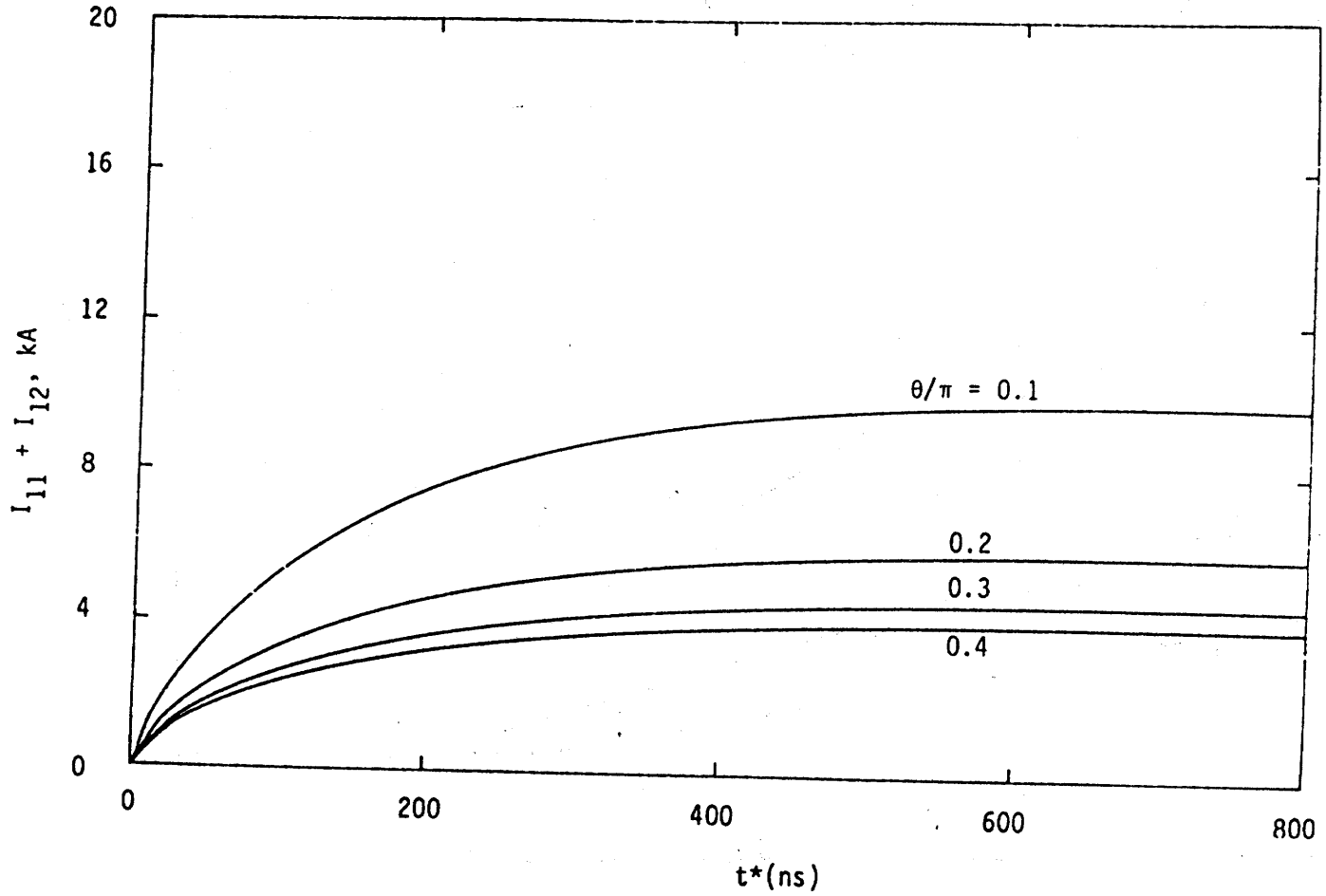

Figure 10. Current induced on conductor #1 by the incident EMP and the scattered field from conductor #2 which is 9 m away from #1 and at the same height as #1 from ground.

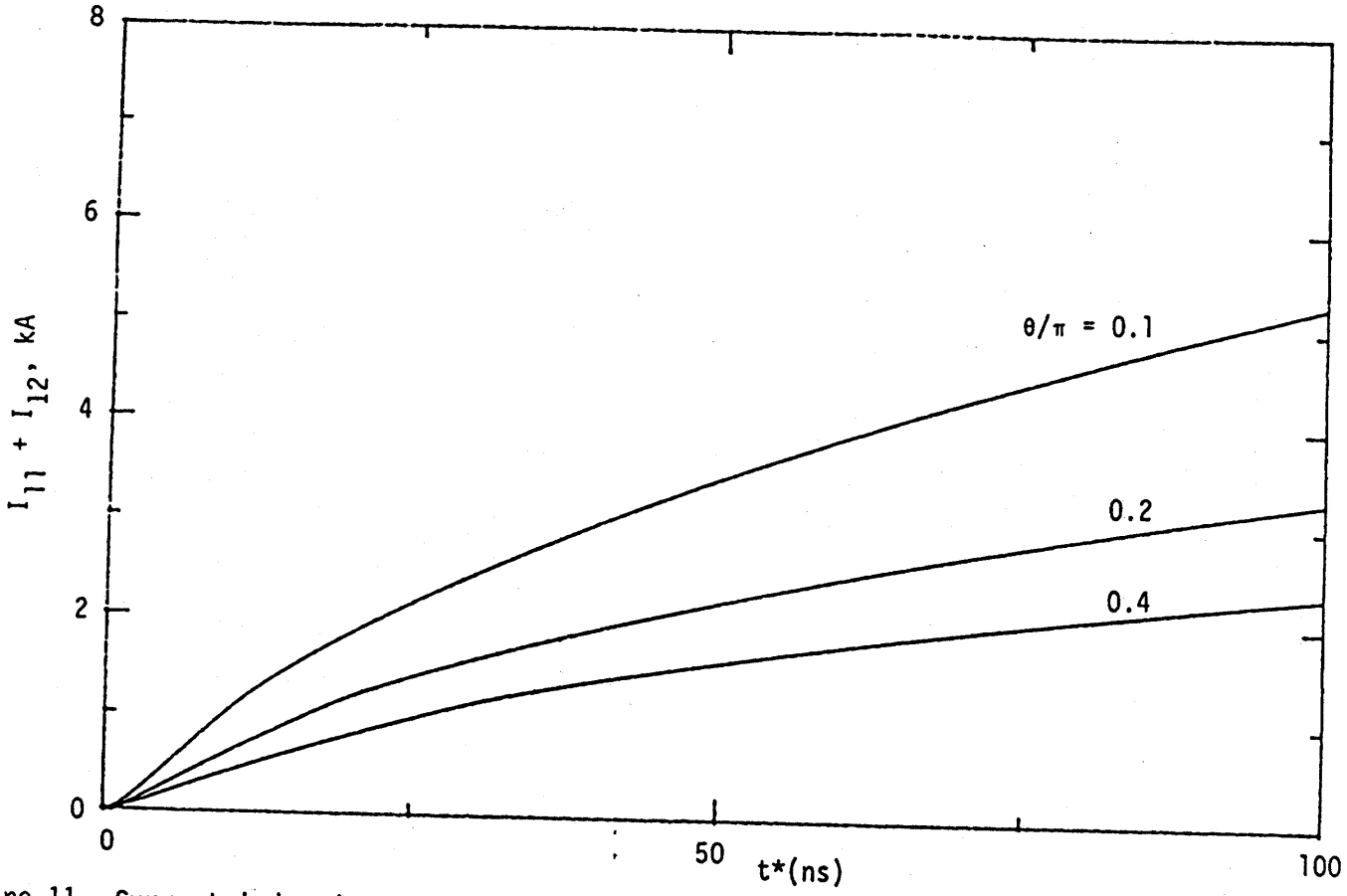

Figure 11. Current induced on conductor #1 by the incident EMP and the scattered field from conductor #2 which is 9 m away from #1 and at the same height as #1 from ground.

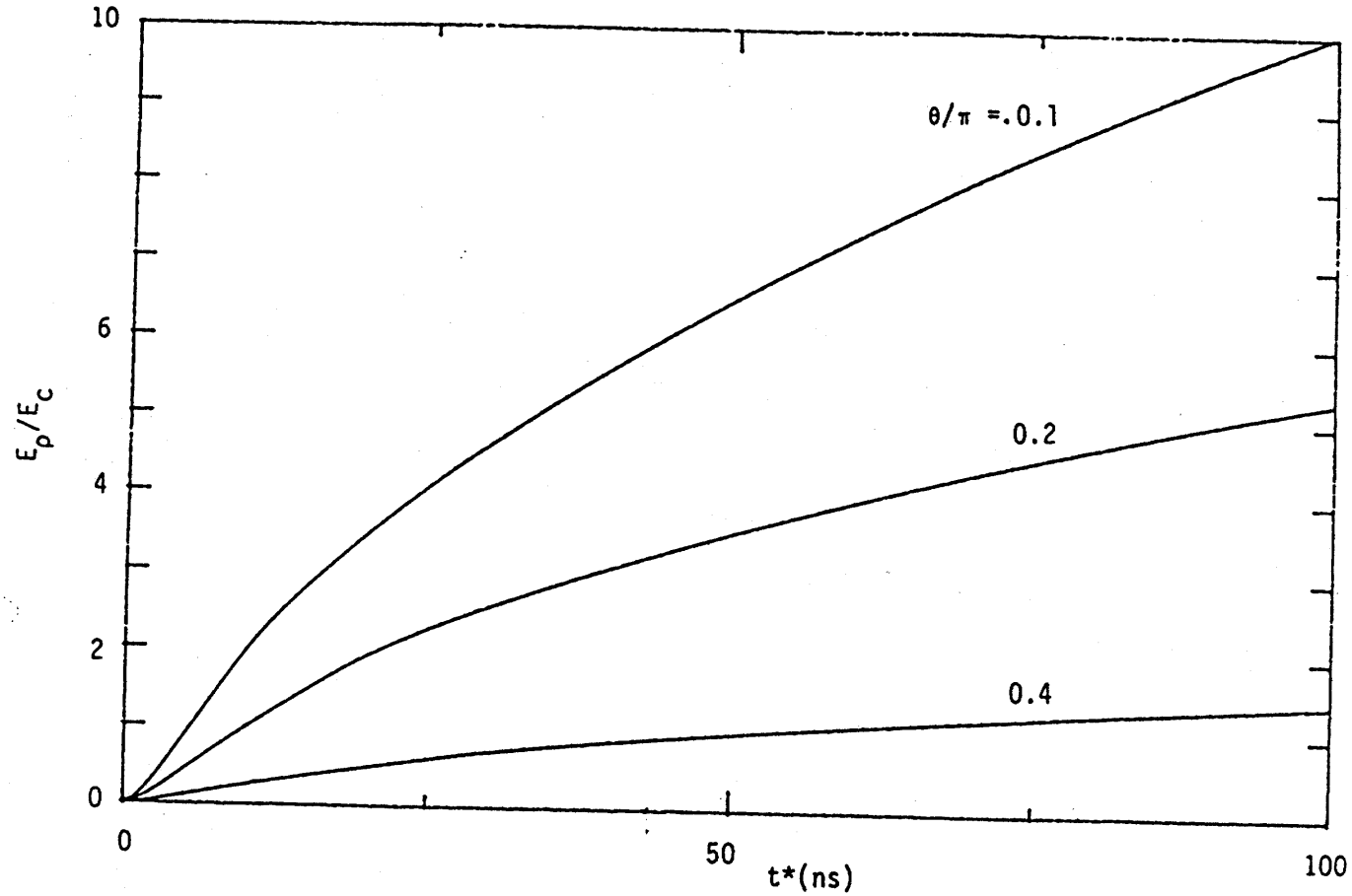

Figure 12. Normalized radial electric field including the effect of scattered field from a neighboring wire 9 m away and at the same height as the other wire.

V. EFFECT OF GROUND REFLECTED FIELD

The fourth term, I_{1g}, of Equation 1 is the current induced on wire #1 due to the incident HEMP reflected by a conducting ground. Using the same technique as in Section III one can immediately write down the result for I_{1g}, namely,

$$I_{1g} \simeq \frac{-E_o}{L(a_1,\ t^*)} \int_0^{t^*} g(t)dt \tag{12}$$

when

$$L(a_1,t^*) = \frac{Z_o}{2\pi c} \sin\theta\ \ell n\left(\frac{2ct^*}{\Gamma a_1 \sin\theta}\right)$$

$t^* = t - t_g$, t_g being defined in Sec. II

$g(t)$ = ground reflected field $= \frac{1}{2\pi j}\int R\tilde{F}e^{st}ds$

with $\tilde{F}$ being the Fourier transform of the incident HEMP and R the Fresnel reflection coefficient for parallel polarization which is given by [9]

$$R = \frac{\varepsilon_r^* \sin\theta - \sqrt{\varepsilon_r^* - \cos^2\theta}}{\varepsilon_r^* \sin\theta + \sqrt{\varepsilon_r^* - \cos^2\theta}} \tag{13}$$

and $\varepsilon_r^* = \varepsilon_r + \sigma/(s\varepsilon_o)$, ε_r being the ground relative dielectric constant and σ the ground conductivity.

Figure 13 is the time history of the ground reflected field for ground conductivity 10^{-2} S/m and 10^{-3} S/m, when the incident HEMP has the electric field vector lying in the plane of incidence. Figure 14 is the time history of the current induced on the wire by the ground reflected field alone, whereas Figures 15 and 16 give the current and radial electric field induced

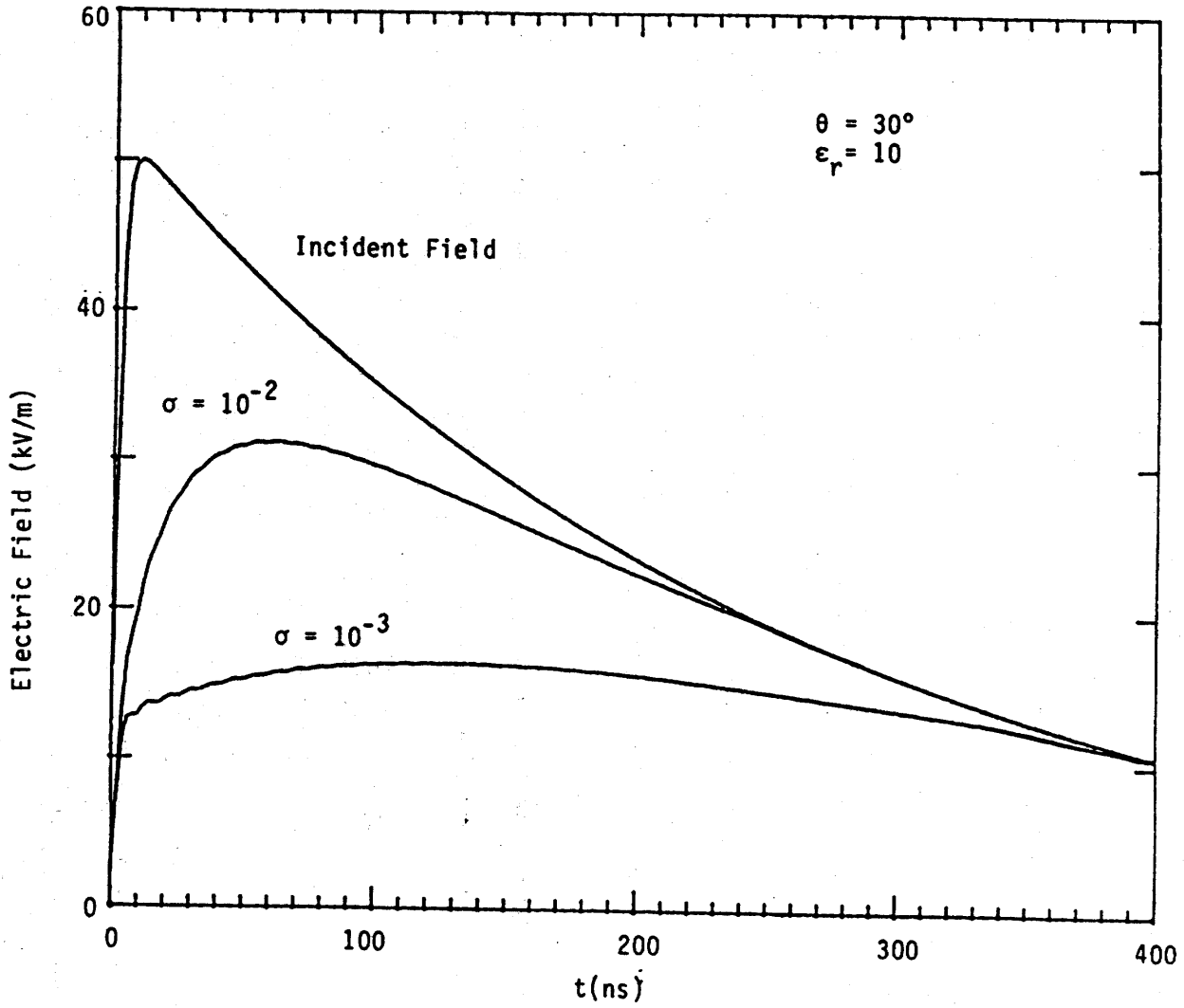

Figure 13. Ground reflected field for ground conductivity $\sigma = 10^{-2}$S/m and $\sigma = 10^{-3}$S/m when the incident field is given by $E_0 = 52.5$kV/m, $\alpha = 4.0 \times 10^6$ sec^{-1}, $\beta = 4.78 \times 10^8$sec^{-1}, and $\theta = 30°$.

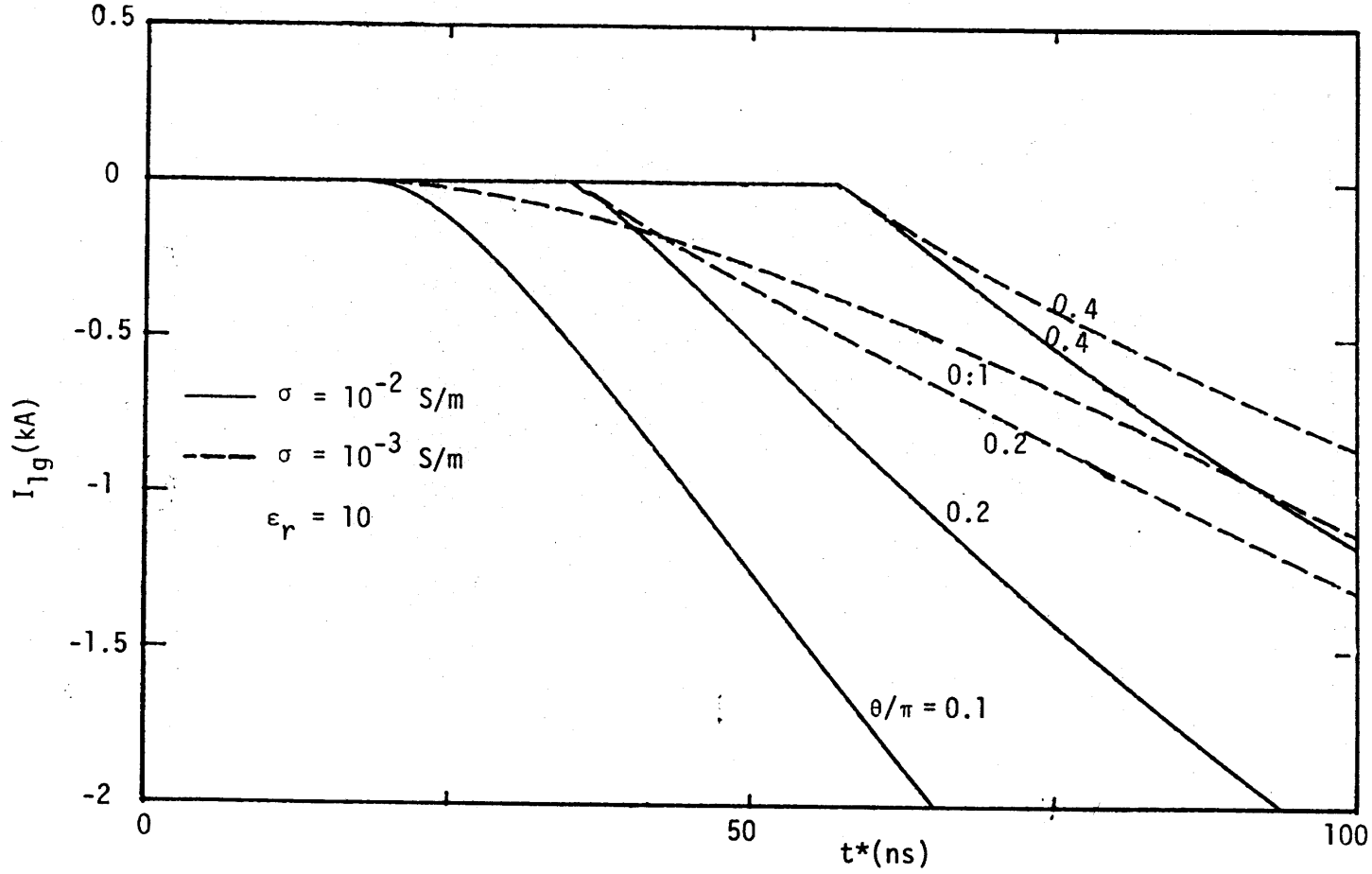

Figure 14. Induced current on conductor # 1 by the ground reflected wave for conductivity σ = 10^{-2} S/m or σ = 10^{-3} S/m.

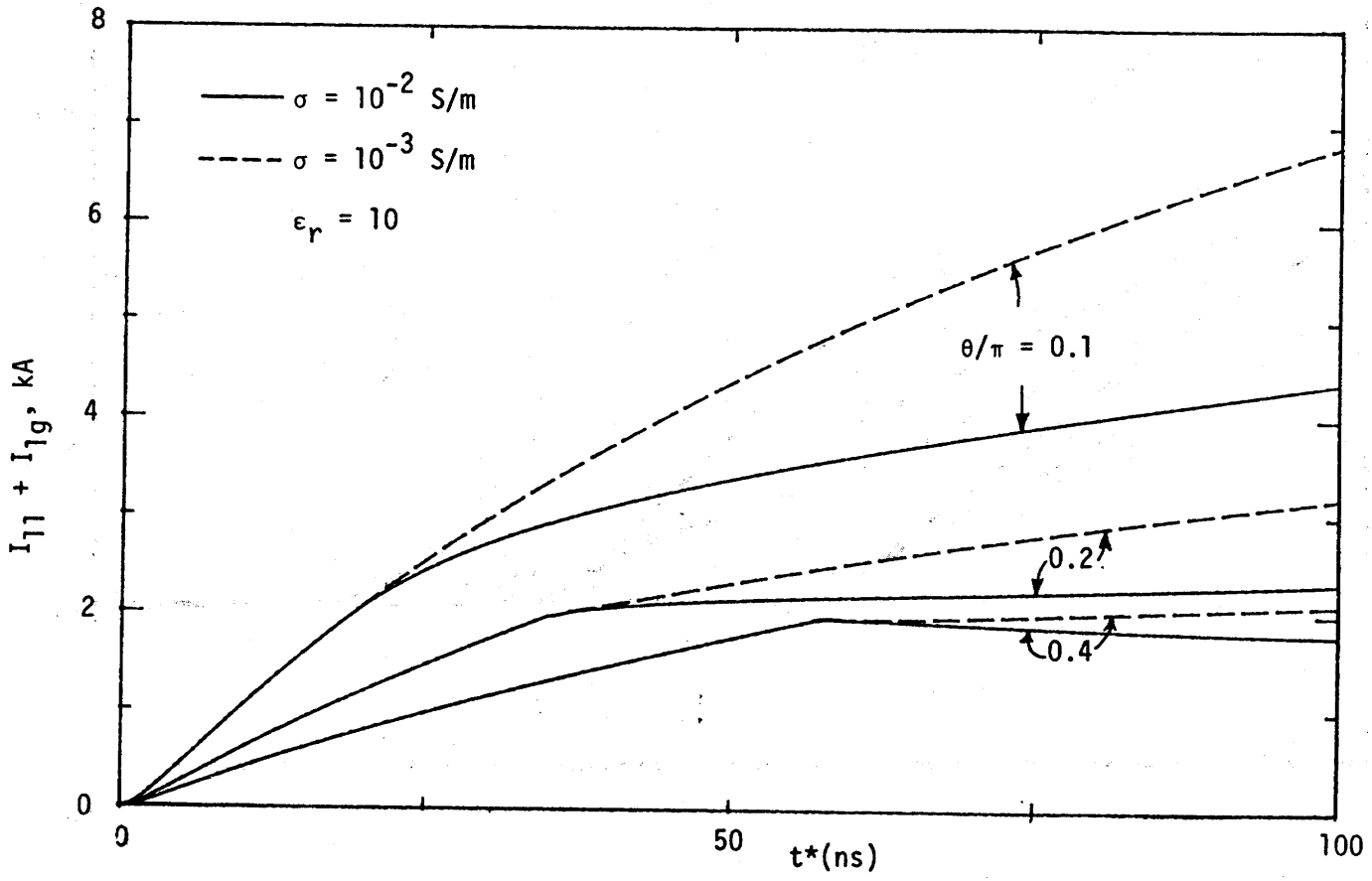

Figure 15. Current induced on wire #1 by the incident EMP and the ground reflected wave for conductivity $\sigma = 10^{-2}$ S/m or $\sigma = 10^{-3}$ S/m.

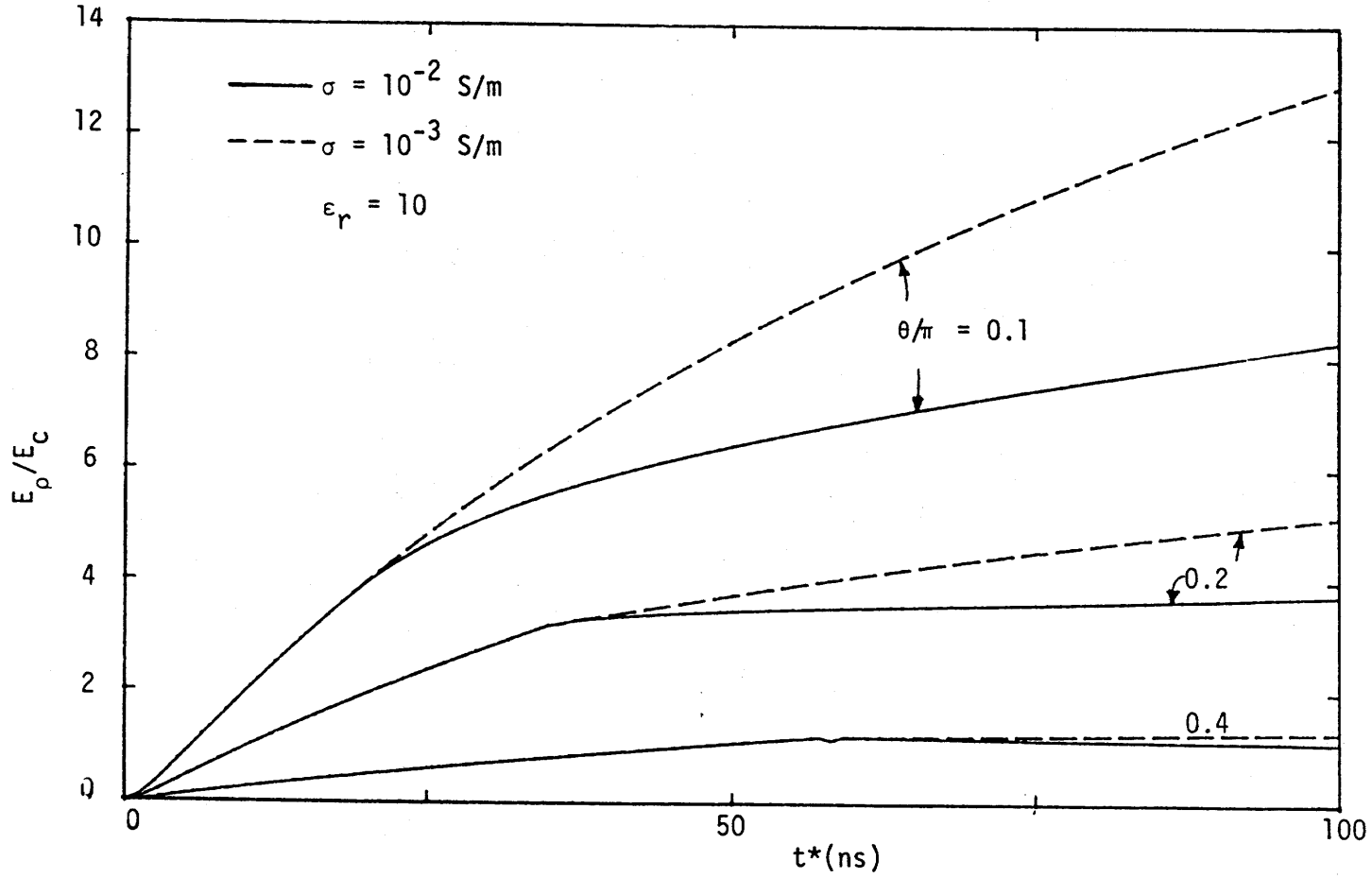

Figure 16. Normalized radial electric field including the effect of the ground reflected field for conductivity $\sigma = 10^{-2}$ S/m or $\sigma = 10^{-3}$ S/m.

by the incident and ground reflected field together. By comparing these figures with Figures 6 and 7 one can get the effect of the ground reflected field. Again, just like the scattered field from a neighboring wire the ground reflected field has a tendancy of decreasing the inducing effect of the incident field.

VI. EFFECT OF WIRE RESISTIVITY

Up to now, the wire's resistivity has been ignored in all the previous sections. Let R' be the resistance of the wire per unit length. Then the boundary condition at the surface of the wire will be

$$E_z^{sc} + E_z^{inc} = IR' \tag{14}$$

and the induced current will have an additional term in Equation 3, namely [10]

$$I_\delta = \frac{2\pi c E_o}{Z_o \sin\theta} \cdot \frac{1}{2\pi j} \int \frac{e^{st}\,ds}{s\{K_o[(sa/c)\sin\theta] + p \csc\theta\, K_1[(sa/c)\sin\theta]\}} \tag{15}$$

with $p = 2\pi a R'/Z_o$, and K_1 being the modified Bessel function of the second kind of the first order. Note that R' has been taken to be the DC resistance of the wire. If the skin effect is taken into account, p in Equation 15 will be replaced by [11]

$$p \to \frac{q}{\sin\theta\,[1 + \sigma_w/(s\varepsilon_o)]} \frac{I_o(saq/c)}{I_1(saq/c)} \tag{16}$$

where $q = \sqrt{\sin^2\theta + \sigma_w/(s\varepsilon_o)}$, σ_w = wire conductivity, and I_1 is the modified Bessel function of the first kind of the first order. Neff has computed $\hat{I}_\delta$, the frequency-domain version of Equation 15, for $p = 2\pi a R'/Z_o$ and for p given by Equation 16 [11]. In his computation, a = 2.03 cm; $\sigma_w = 3.54 \times 10^7$ S/m; $\theta = 90°, 54°, 36°, 18°, 6°$; and the frequency ranges from 0.16 Hz to 1.59 GHz. He found practically no difference between the two expressions except for the case $\theta = 6°$ and the frequency is from a few Hz to a few kHz, in which case the difference in amplitude is about 5% and in phase

angle less than 10°.

Equation 15 can be approximated in the same manner as described in Section III. Instead of the expression given by Equation 4, it now takes the form

$$I_\delta \simeq \frac{E_o}{L} \exp\left(-\frac{R}{L}t^*\right)u(t^*) \qquad (17)$$

where $R = R'/\sin\theta$ and L is given in Equation 4. Equation 17 can be time-convolved with the incident HEMP double-exponential waveform and the resulting expression is dotted in Figure 17 along with the case of a perfectly conducting wire. In the figure, R' is chosen for $\sigma_w = 3.54 \times 10^7$ S/m (copper wire), a = 0.715 cm (0.28"), and the current assumed to flow within a skin depth, which at 100 MHz is about 0.8×10^{-3} cm (0.31 mil). Thus, one obtains $R' \simeq 8 \times 10^{-2}$ Ω/m, about three orders of magnitude larger than the wire's DC resistance. It can be concluded from the figure that the wire resistivity has practically no effect on the induced current and radial electric field.

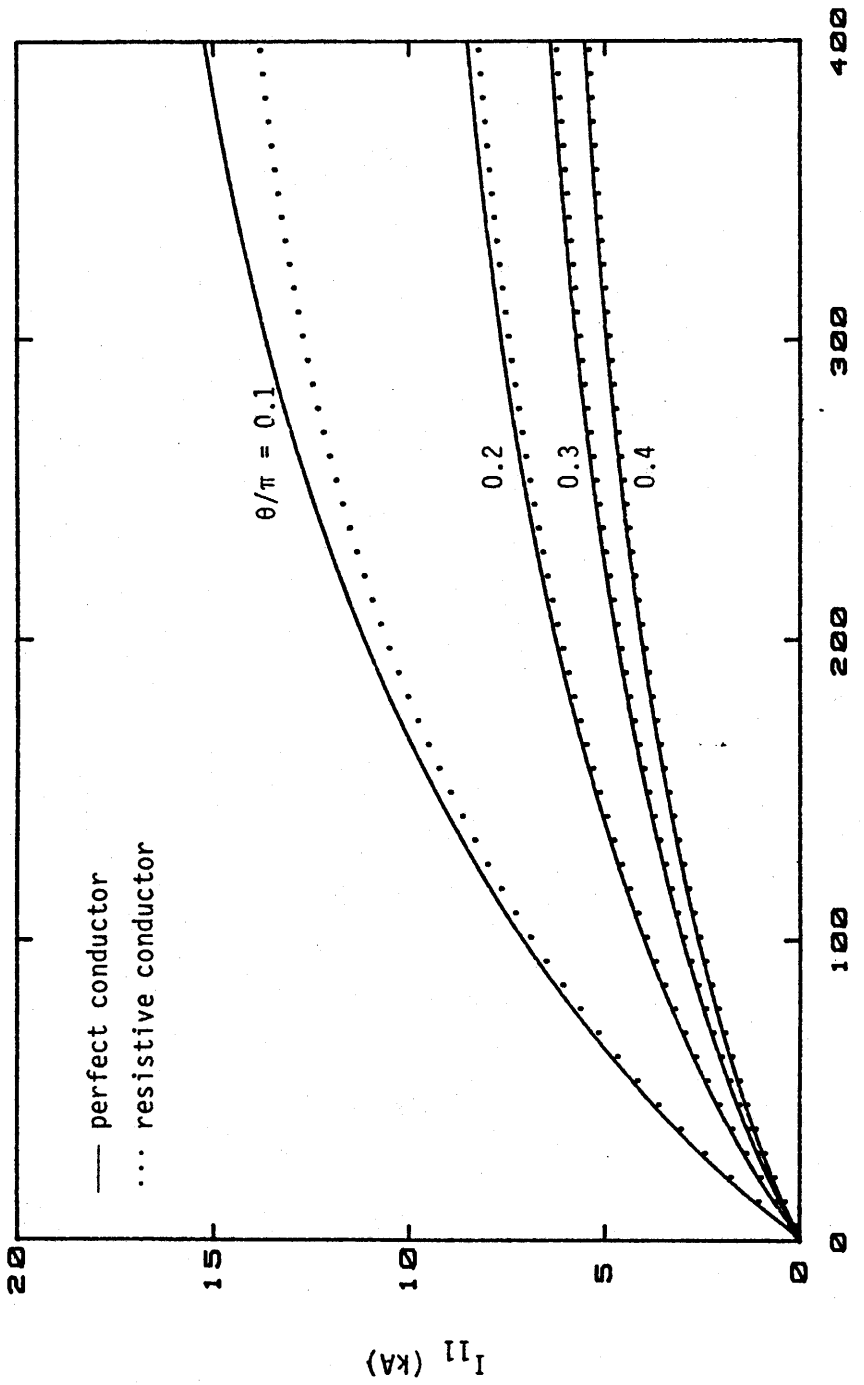

Figure 17. Effect of conductor's resistivity on induced current for $R' = 8 \times 10^{-2}$ Ω/m and a = 0.715 cm.

VII. THE COMBINED EFFECT

In Sections III through VI various effects and their relative importance are discussed regarding their ability in inducing currents and radial electric fields on a multi-conductor line over a finitely conducting ground. In this section these various effects will be added up with appropriate time delays for a two-wire system over a ground.

Figure 18 is the time history of the total induced current on either wire #1 or wire #2. The curves were obtained based on a linear, time-domain, single scattering theory, as has been discussed in Section II. The mark "+" on each curve indicates the time when the second scattering contributes "positively" to the induced current just as the direct incident field. The curves beyond the marks "+" should be somewhat higher than those shown. Nevertheless, one expects the peak induced current will be somewhere around 2 kA to 6 kA depending on the angle of incidence.

Figure 19 is the time history of the corresponding radial electric field. Just like the induced current, the ground conductivity has a more pronounced effect for a smaller angle of incidence. The incident HEMP waveform for both figures is

$$E = 52.5[\exp(-4 \times 10^6 t) - \exp(-4.78 \times 10^8 t)], \text{ (kV/m)} \qquad (18)$$

with $\vec{E}$ and the wires being parallel to the plane of incidence, which is formed by the vector $\vec{k}$ and the vector normal to the air-ground interface.

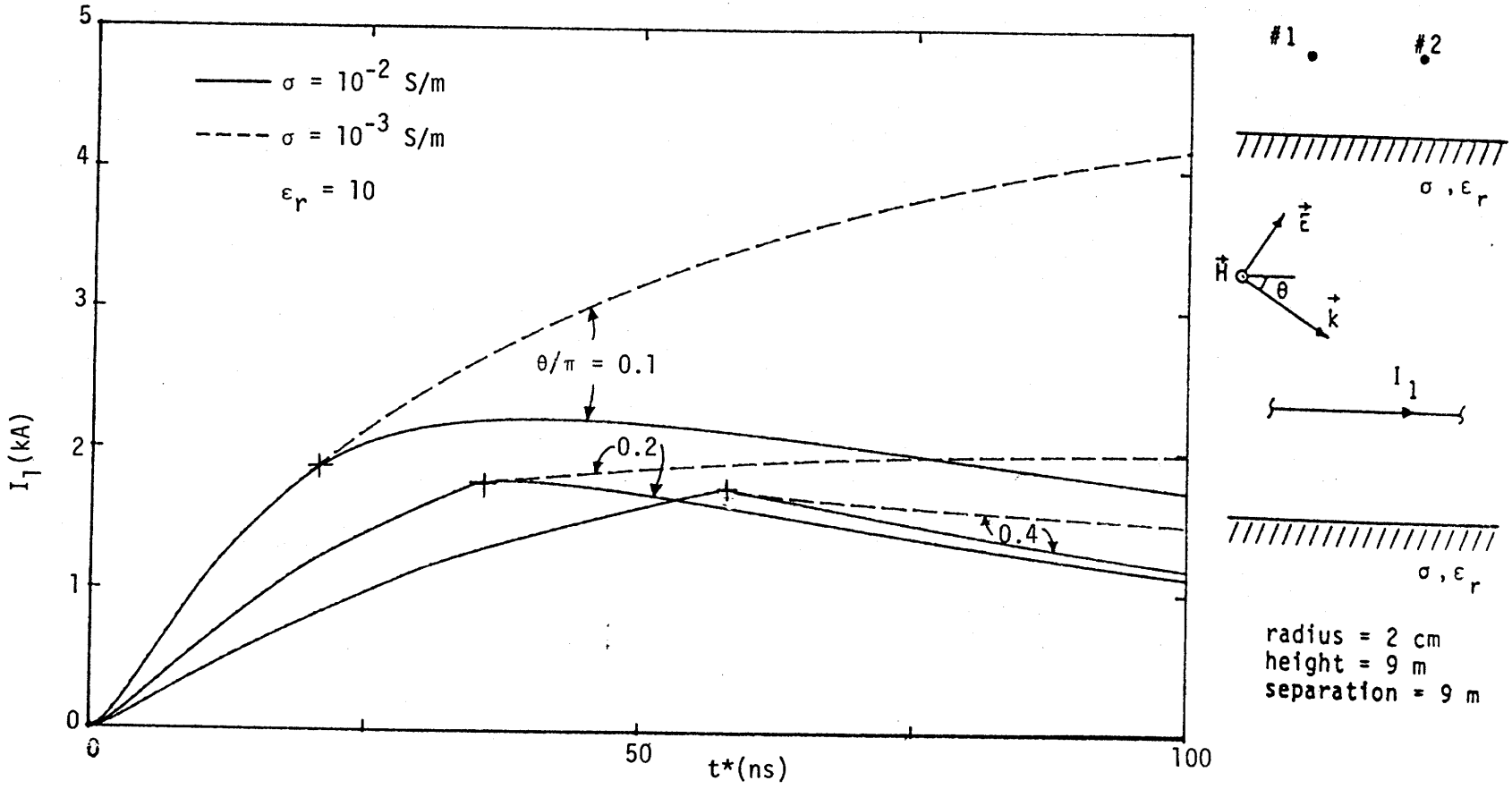

Figure 18. Total current induced on conductor #1 which is 9 m away from conductor #2 and at the same height as #2 from ground for conductivity $\sigma = 10^{-2}$ S/m or $\sigma = 10^{-3}$ S/m. At "+", a multiple scattered field will arrive at wire #1.

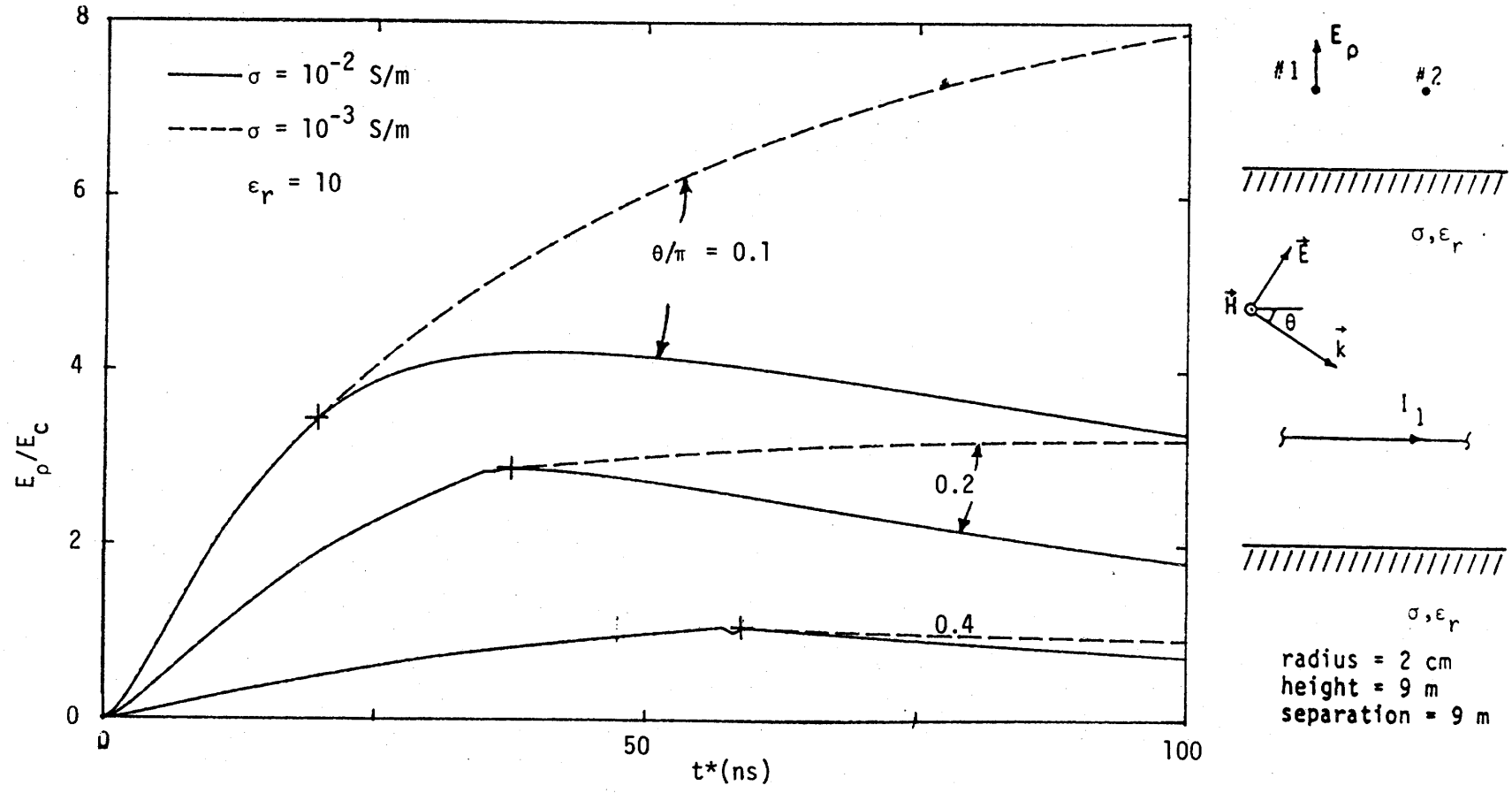

Figure 19. Total normalized radial electric field induced on wire #1 which is 9 m away from wire #2 and at the same height as wire #2 for conductivity $\sigma = 10^{-2}$ S/m or $\sigma = 10^{-3}$ S/m. At "+", a multiple scattered field will arrive at wire #1.

VIII. APPLICATIONS

The techniques described in the preceding sections will now be applied to two typical line configurations: (1) a typical 3ϕ 765 kV single-circuit transmission line, and (2) a typical 3ϕ 13.2 kV single-circuit distribution line. The cross-sectional views of these two lines are shown in Figure 20. The results to be described below correspond to a HEMP waveform given by Equation 18 with the same polarization and angle of incidence as those of Figures 18 and 19.

The results of calculation for the peak values of I, $\dot{I}$, E_ρ, $\dot{E}_\rho$ are summarized in Table 1. Figures 21 through 32 give the time variations of the induced current and radial electric field on all the shield wires and phase conductors. In the 765 kV case an equivalent conductor was used to approximate a group of four conductors using the geometric-mean formula for the equivalent radius, the value of which is shown in Figure 20. Note that due to symmetry, phase conductors #3 and #5 have the same response, and so do shield wires #1 and #2.

In the case of the 765 kV line Table 1 shows that the peak induced current is about 2 to 3 kA on each phase conductor and shield wire, whereas the peak rate of rise of the current is about 10^{11} A/s, comparable to the most severe lightning return stroke. Unlike the lightning case where the effect is relatively localized, the HEMP effect is quite widespread, however. The induced electric field (voltage gradient) on the shield wire can be a few tens of MV/m, while on the phase conductors it is only a few tenths of MV/m.

In the case of the 13.2 kV distribution line the peak current is a few tenths of kA and its peak rate of rise is a few tens of 10^{10} A/s. The radial electric field is a few MV's per meter. It can be seen that the proximity of the phase conductors tends to alleviate the inducing effect of HEMP.

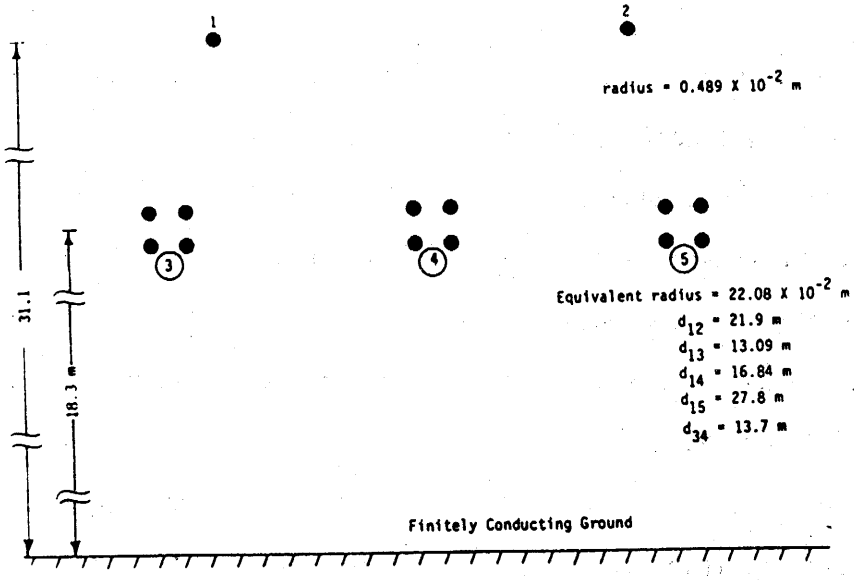

A typical configuration of a 3ϕ 765 kV single-circuit transmission line

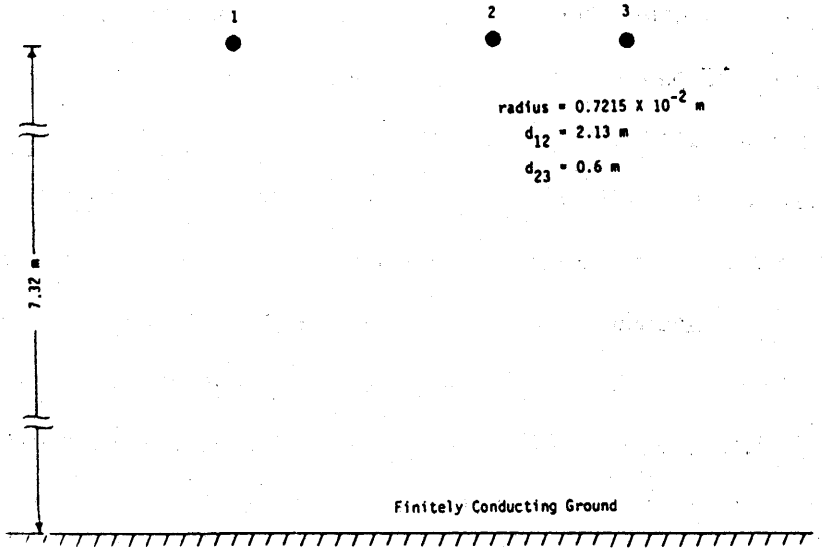

A tyoical configuration of a 3ϕ 13.2 kV distribution line

Figure 20. Two typical line configurations.

TABLE 1. SUMMARY OF (PEAK) HEMP RESPONSES FOR TWO TYPICAL LINE CONFIGURATIONS

765 kV TL

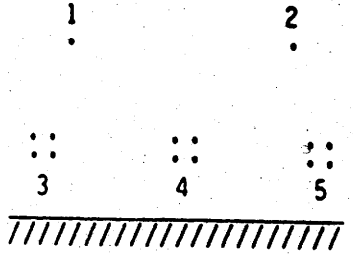

Wire \ Quantity / θ		I (kA)	$\dot{I}$ (kA/μs)	E_ρ (MV/m)	$\dot{E}_\rho$ (MV/m/μs)
#1	18°	2.5	95	20	1140
	72°	2.5	30	7	113
#3	18°	2.5	160	0.4	42
	72°	2.5	70	0.2	5.7
#4	18°	2.0	160	0.4	45
	72°	2.0	70	0.1	6

12 kV DL

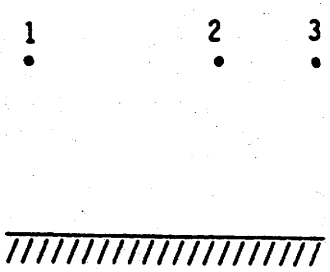

Wire \ Quantity / θ		I (kA)	$\dot{I}$ (kA/μs)	E_ρ (MV/m)	$\dot{E}_\rho$ (MV/m/μs)
#1	18°	0.7	80	4	675
	72°	0.7	40	1	83
#2	18°	0.3	50	2	375
	72°	0.3	30	0.7	75
#3	18°	0.4	50	2	375
	72°	0.4	30	0.7	75

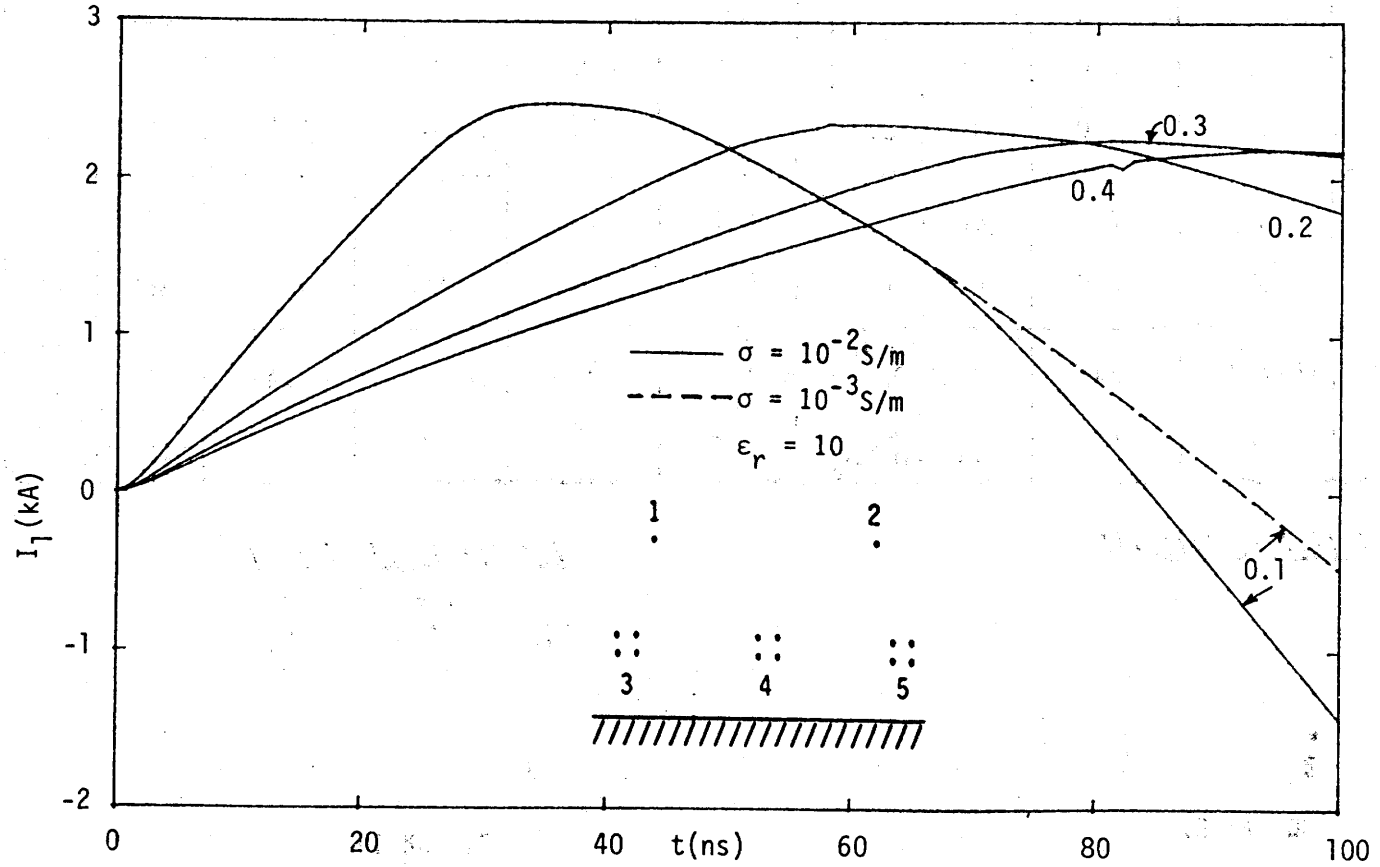

Figure 21. Total current induced on shield wire #1 for ground conductivity $\sigma = 10^{-2}$ S/m or $\sigma = 10^{-3}$ S/m.

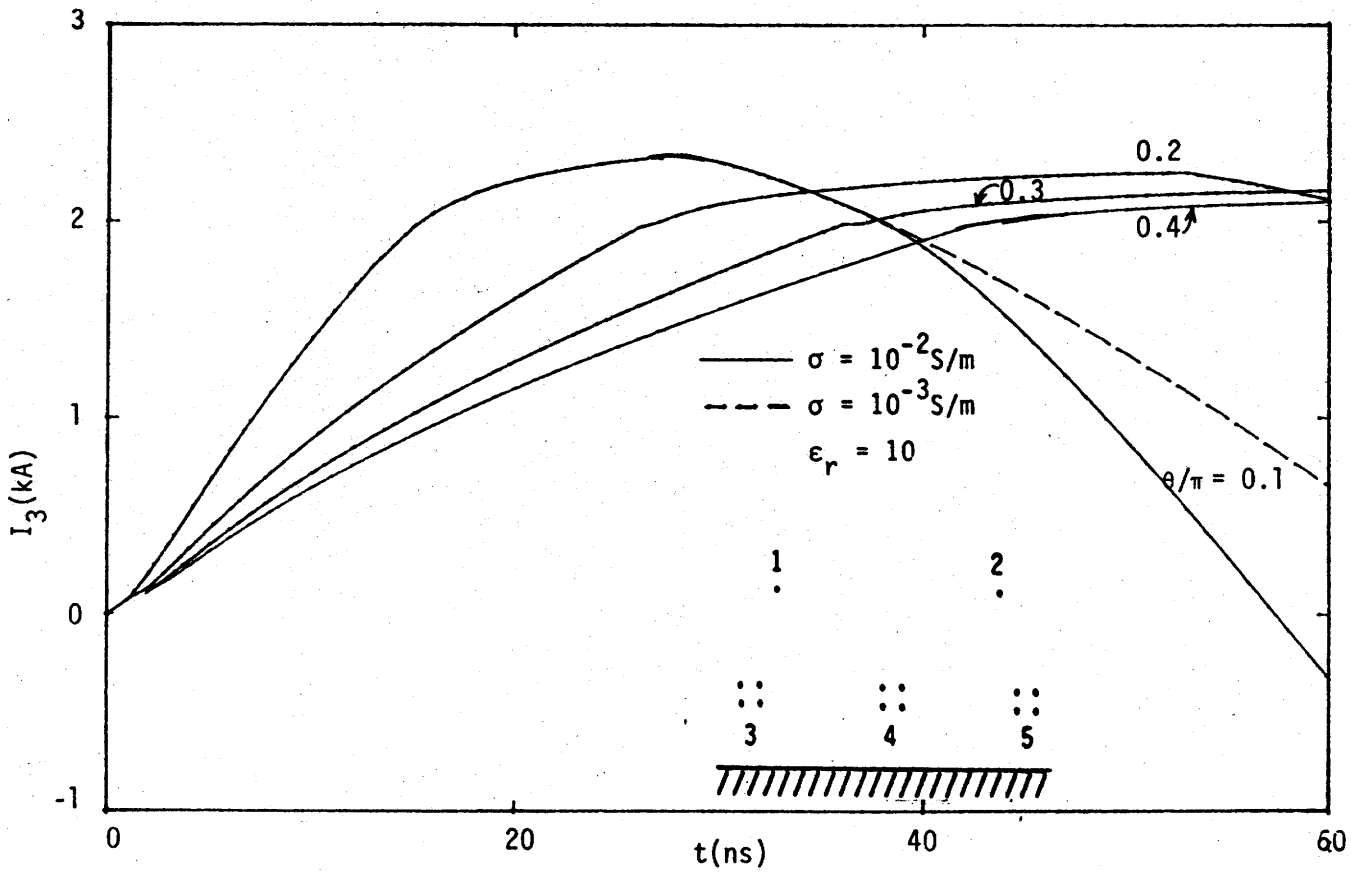

Figure 22. Total current induced on phase wire #3 for ground conductivity $\sigma = 10^{-2}$ S/m or $\sigma = 10^{-3}$ S/m.

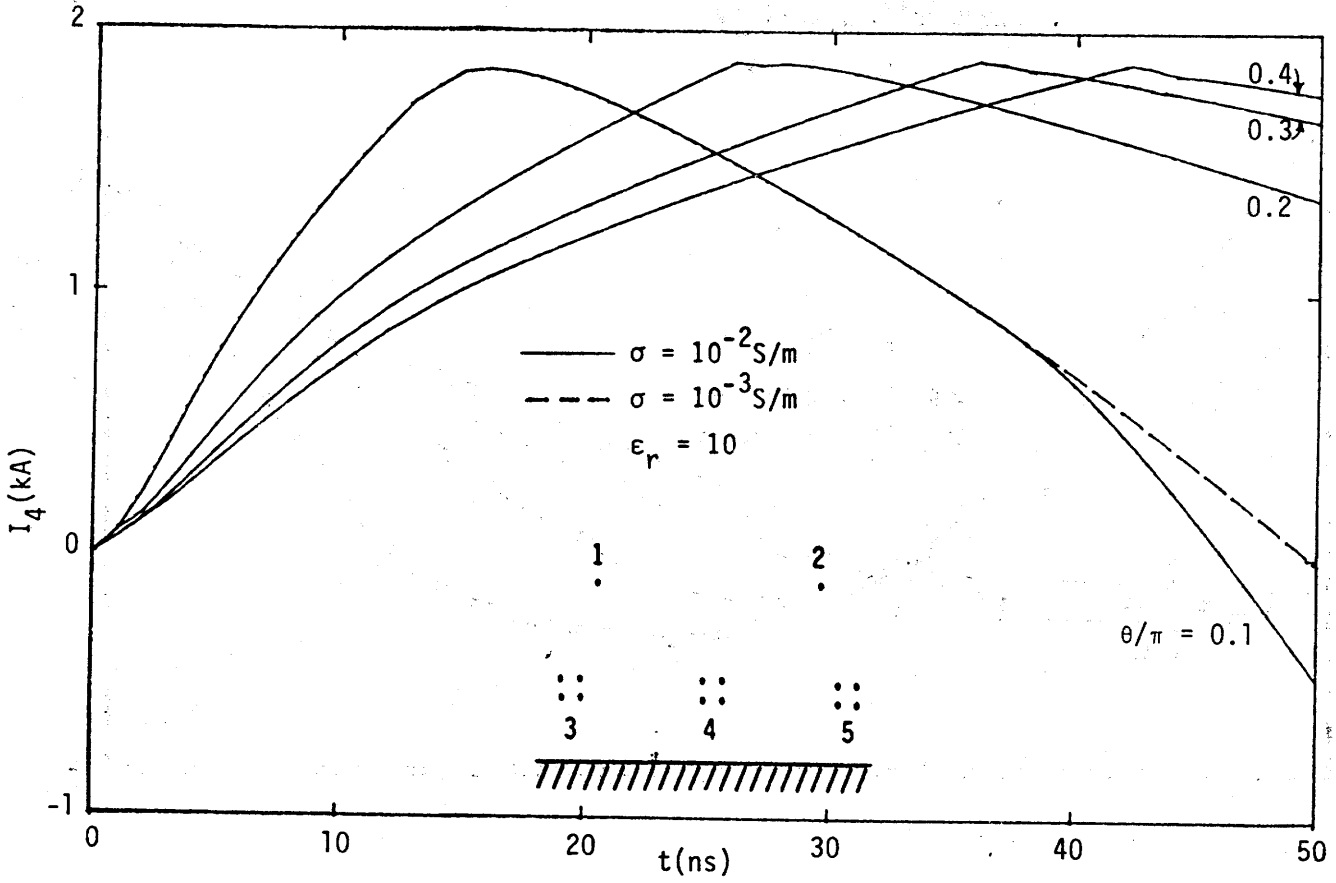

Figure 23. Total current induced on phase wire #4 for ground conductivity $\sigma = 10^{-2}$ S/m or $\sigma = 10^{-3}$ S/m.

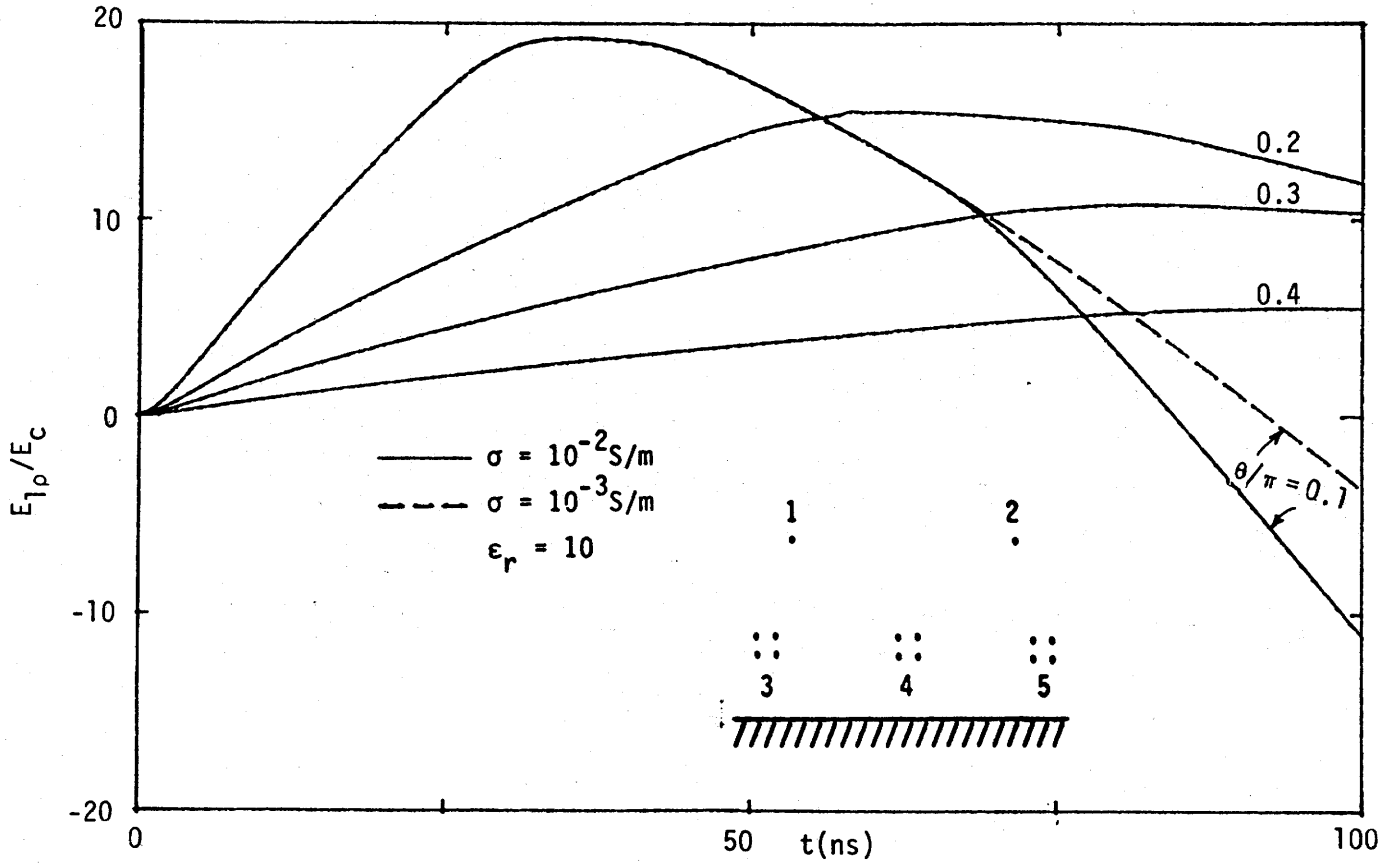

Figure 24. Total normalized radial electric field induced on shield wire #1 for ground conductivity $\sigma = 10^{-2}$ S/m or $\sigma = 10^{-3}$ S/m.

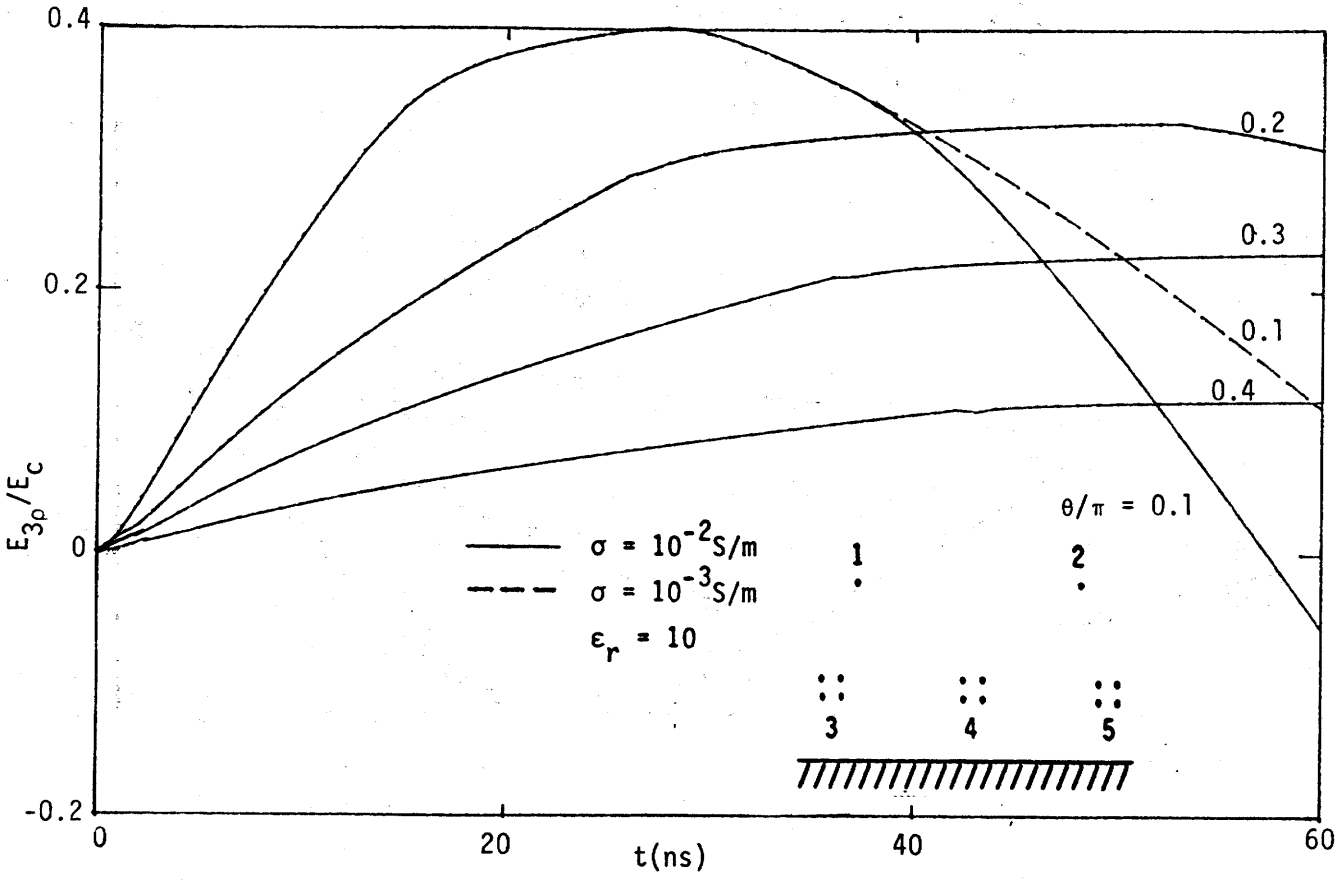

Figure 25. Total normalized radial electric field induced on phase wire #3 for ground conductivity $\sigma = 10^{-2}$ S/m or $\sigma = 10^{-3}$ S/m.

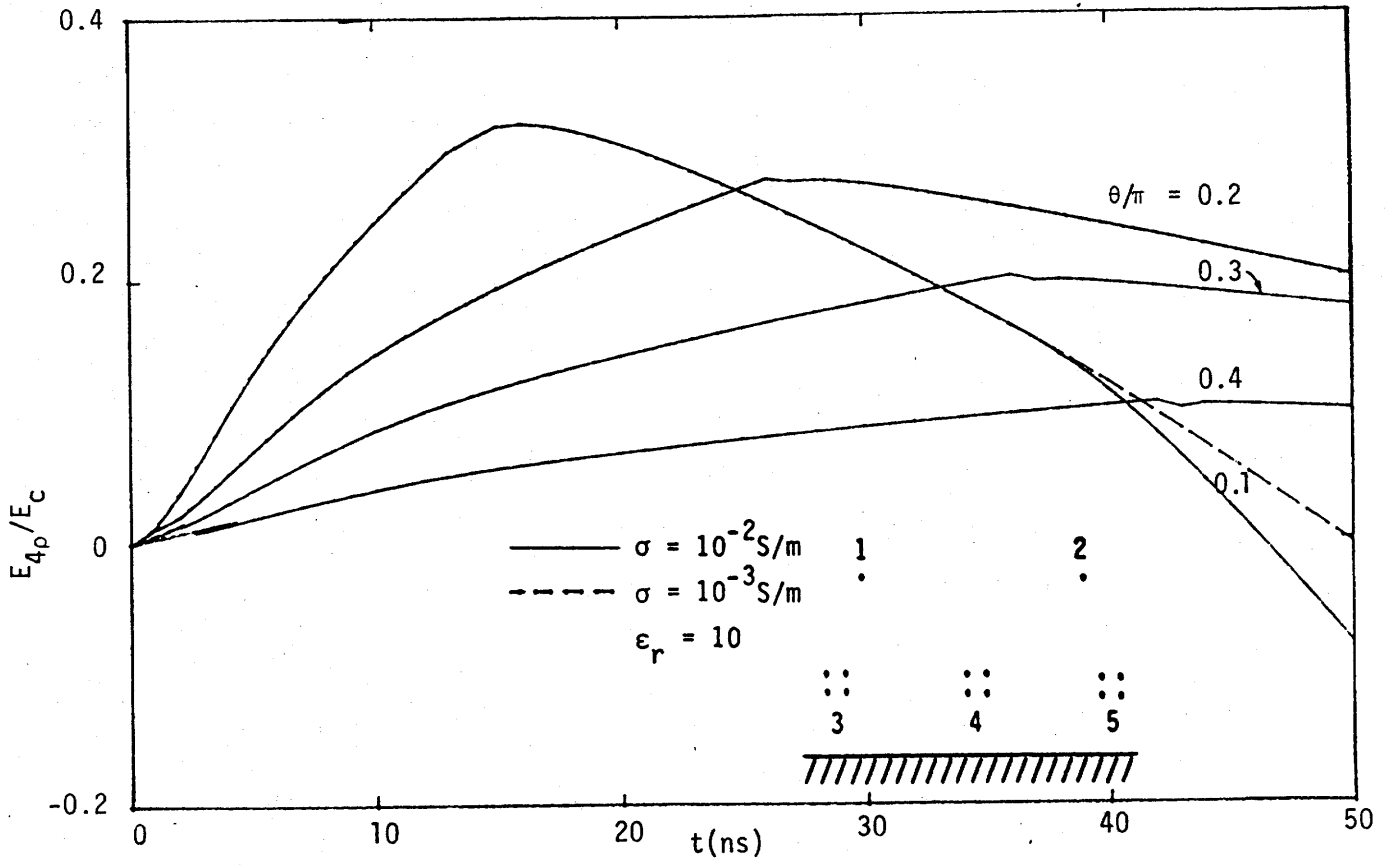

Figure 26. Total normalized radial electric field induced on phase wire #4 for ground conductivity $\sigma = 10^{-2}$ S/m or $\sigma = 10^{-3}$ S/m.

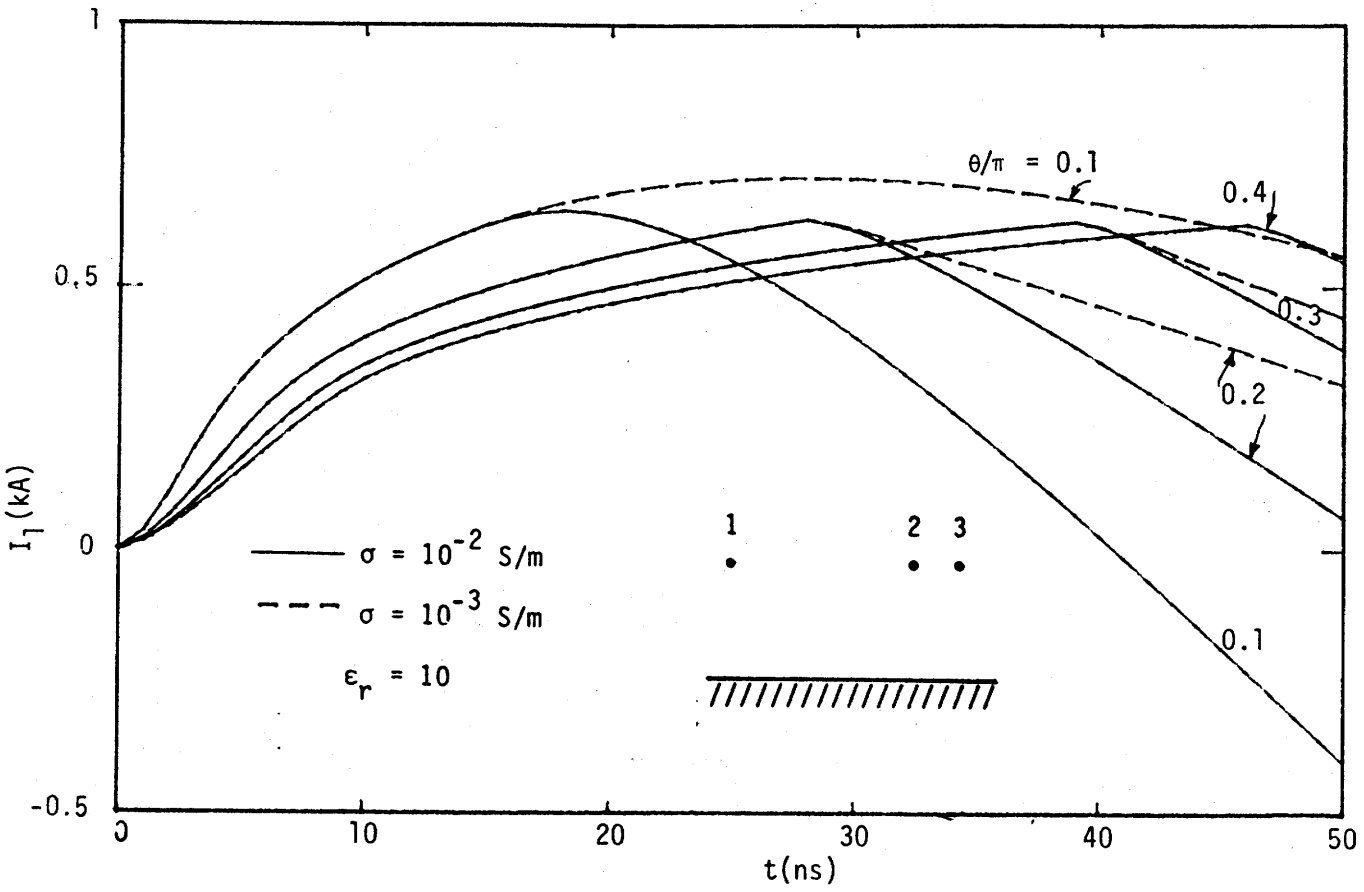

Figure 27. Total current induced on phase wire #1 for ground conductivity $\sigma = 10^{-2}$ S/m or $\sigma = 10^{-3}$ S/m.

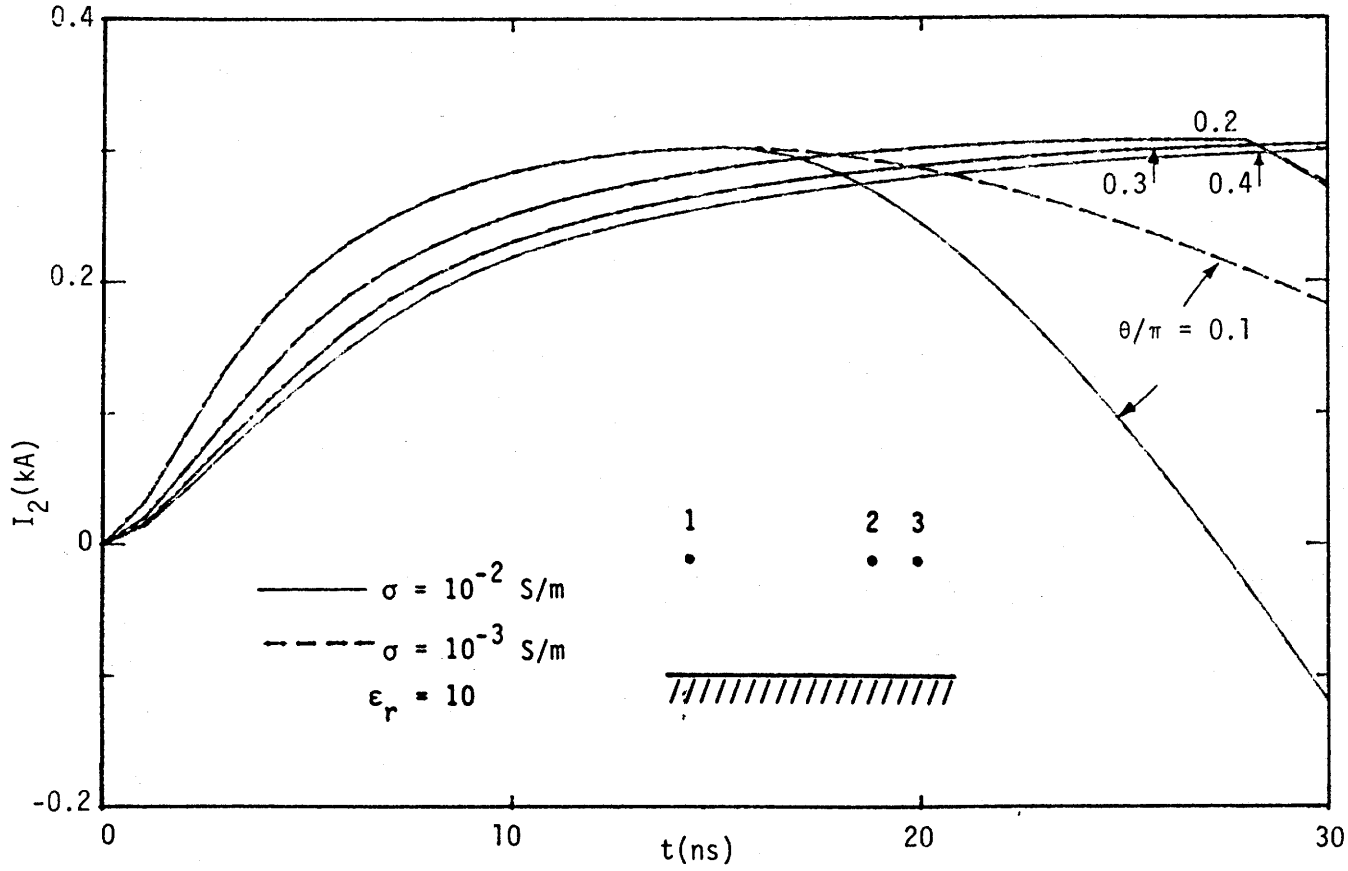

Figure 28. Total current induced on phase wire #2 for ground conductivity $\sigma = 10^{-2}$ S/m or $\sigma = 10^{-3}$ S/m.

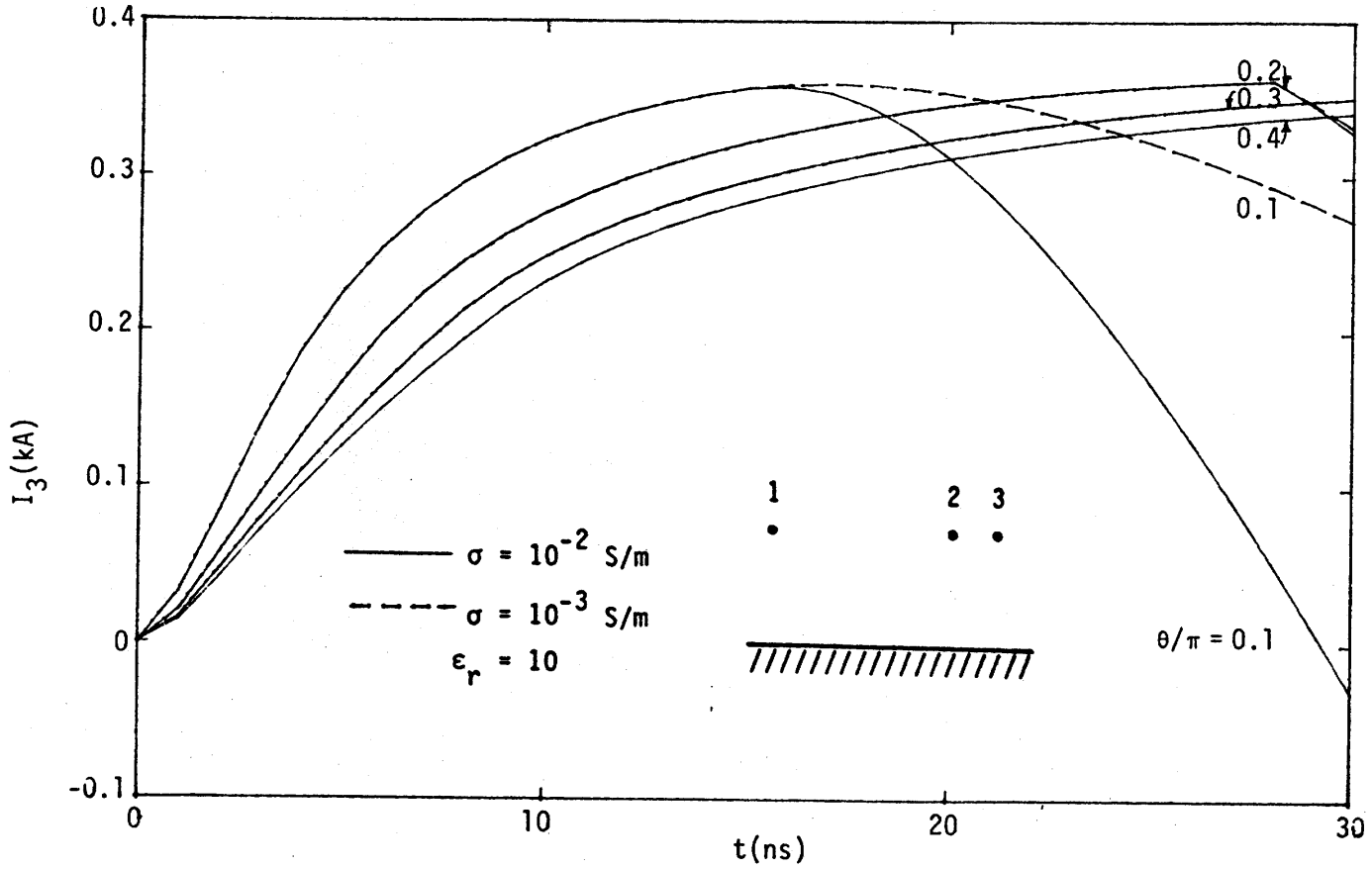

Figure 29. Total current induced on phase wire #3 for ground conductivity $\sigma = 10^{-2}$ S/m or $\sigma = 10^{-3}$ S/m.

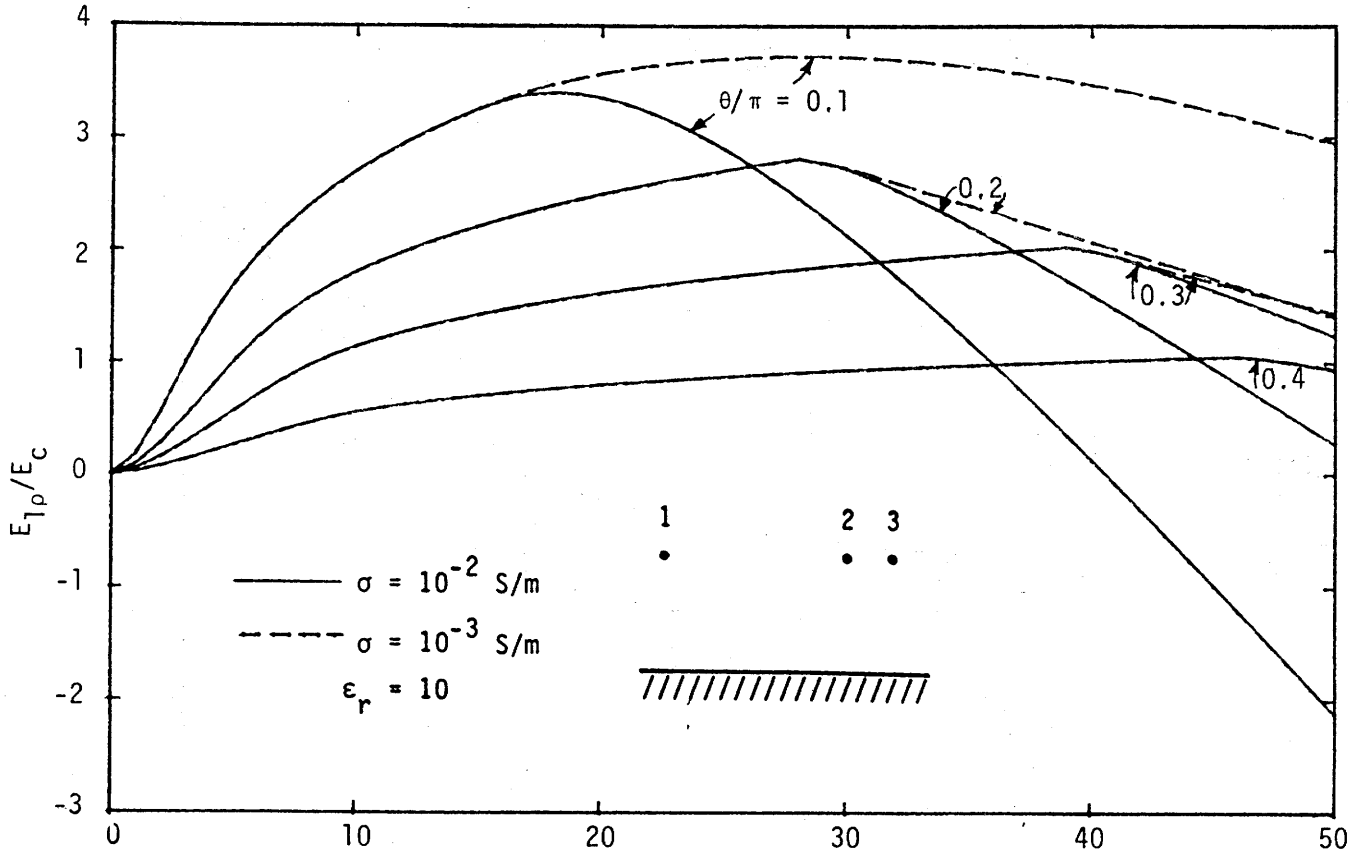

Figure 30. Total normalized radial electric field induced on conductor #1 for ground conductivity $\sigma = 10^{-2}$ S/m or $\sigma = 10^{-3}$ S/m.

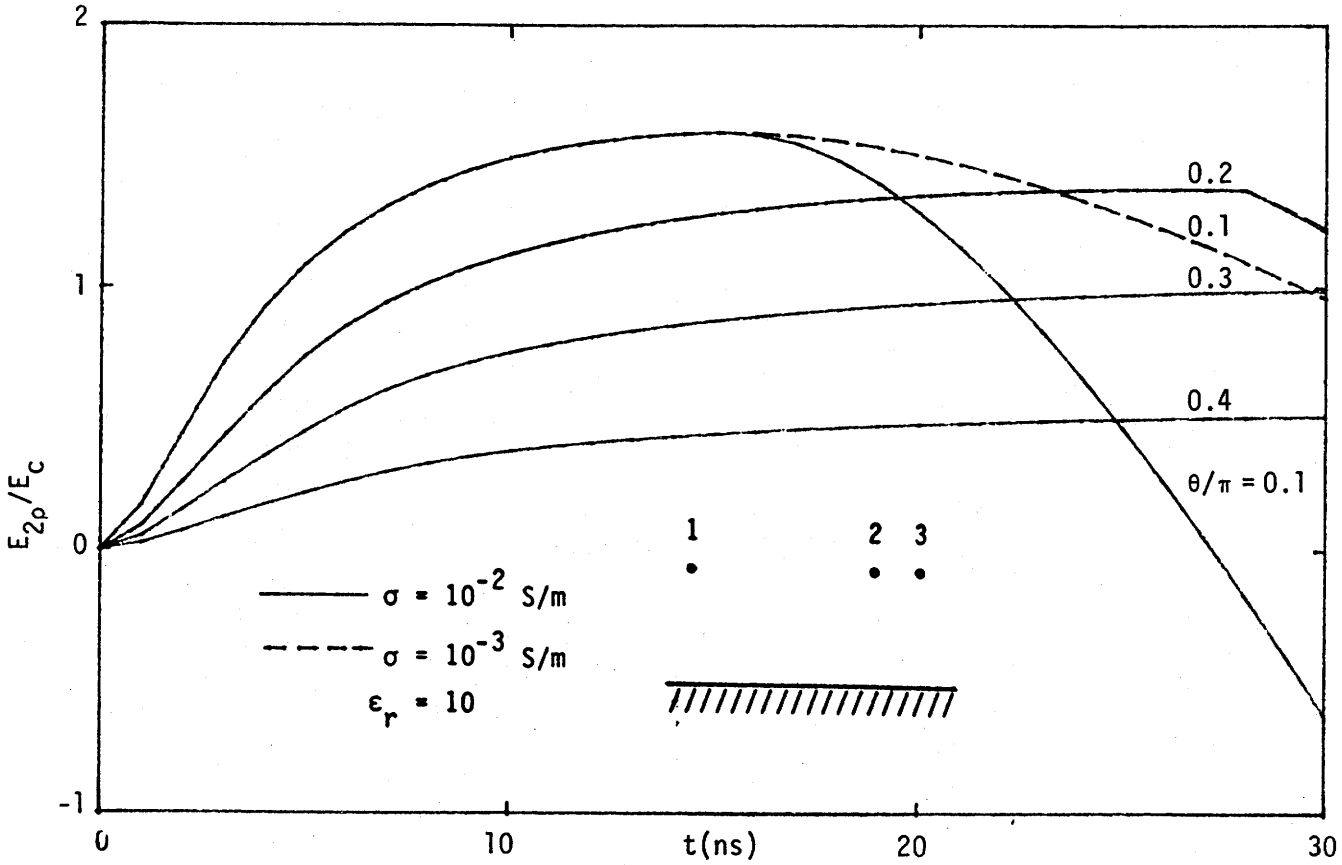

Figure 31. Total normalized radial electric field induced on conductor #2 for ground conductivity $\sigma = 10^{-2}$ S/m or $\sigma = 10^{-3}$ S/m.

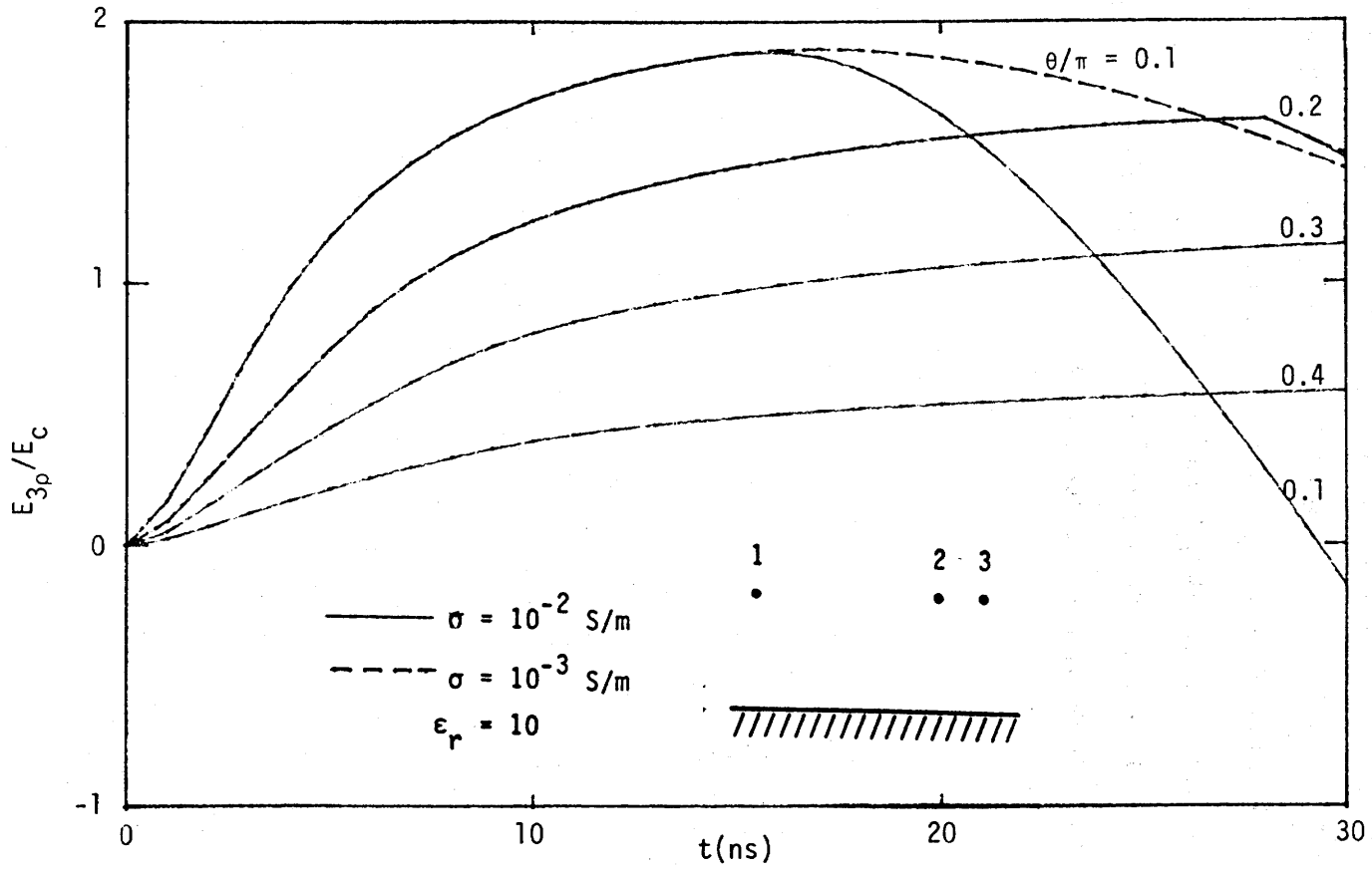

Figure 32. Total normalized radial electric field induced on conductor #3 for ground conductivity $\sigma = 10^{-2}$ S/m or $\sigma = 10^{-3}$ S/m.

For both lines the peak rate of rise of the voltage gradient is quite large, on the order of 10^9 MV per meter per second. What effect such a large value might have on an electric power system need be investigated.

It should be recalled that the foregoing results were derived from a linear, time-domain, single scattering theory. Discontinuities such as stations, towers, etc. along the line have been ignored. Nor have any nonlinear effects, such as corona and flashover, been included. Furthermore, it should also be noted that the results presented are for $\theta \geq 18°$. When the angle θ gets smaller, the effects of multiple scattering from the neighboring wires and the ground will come into play sooner. To account for these effects will require a greater effort.

REFERENCES

1. K.S.H. Lee, editor, EMP Interaction: Principles, Techniques, Reference Data, EMP Interaction 2-1, AFWL, Kirtland AFB, NM, December 1980.

2. E.F. Vance, Electromagnetic Pulse Handbook for Electric Power System, DNA 3466F, Defense Nuclear Agency, Washington, D.C., December 1974.

3. J.R. Carson, "Wave Propagation in Overhead Wires With Ground Return," Bell System Technical Journal, Vol. 5, pp. 539-554, 1926.

4. R.W.P. King, T.T. Wu and L-C Shen, "The Horizontal Wire Antenna Over a Conducting or Dielectric Half-Space: Current and Admittance," Radio Science, 9, no. 7, pp. 701-709, July 1974.

5. C. Flammer and H.E. Singhaus, "The Interaction of Electromagnetic Pulses With an Infinitely Long Conducting Cylinder Above a Perfectly Conducting Ground," Interaction Notes, IN 144, AFWL, Kirtland AFB, NM, July 1973.

6. D.C. Chang and R.G. Olsen, "Excitation of an Infinite Antenna Above a Dissipative Earth," Radio Sciences, 10, no. 8,9, pp. 823-831, August-September 1975.

7. Transmission Line Reference Book, 345 kV and Above, 2nd edition, Electric Power Research Institute, Palo Alto, CA, 1982.

8. P.R. Barnes, "The Axial Current Induced on an Infinitely Long, Perfectly Conducting, Circular Cylinder in Free Space by a Transient Electromagnetic Plane Wave," Interaction Notes, IN 64, AFWL, Kirtland AFB, NM, March 1971.

9. C.E. Baum, "The Reflection of Pulsed Waves from the Surface of a Conducting Dielectric," Theoretical Notes, TN25, AFWL, Kirtland AFB, NM, February 1967.

10. R.W. Latham and K.S.H. Lee, "Radiation of an Infinite Cylindrical Antenna with Uniform Resistive Loading," Sensor and Simulation Notes, SSN83, AFWL, Kirtland AFB, NM, April 1969.

11. H. Neff, Private Communication.

12. B.W. McConnell, "Modeling the Effects of Corona on Electric Power Line Surges Induced by Electromagnetic Pulse," IEEE Conference on Nuclear Radiation Effects, Gatlinburg, TN, July 1983.

APPENDIX

EFFECT OF CORONA

Consider a wire of radius a at a height h above the ground (Fig. 33a). An electromagnetic pulse with parallel polarization is incident on this wire. Current, charges and hence radial electric field on the wire are generated. If the intensity of the induced field exceeds E_c, the corona onset value, the corona discharge will take place around the wire. This phenomenon affects the propagation of the pulse and the scattered wave along the wire and consequently affects the induced current and voltage gradient on the wire.

To quantify this phenomenon, one starts with Maxwell's equations for the fields together with the continuity equations for the charge particles (Ref. 12):

$$\nabla \times \vec{E} = -\mu_o \frac{\partial \vec{H}}{\partial t}$$

$$\nabla \times \vec{H} = \varepsilon_o \frac{\partial \vec{E}}{\partial t} + e(K_e N_e + K_+ N_+ + K_- N_-)\,\vec{E}$$

$$\nabla \cdot \vec{E} = \frac{e}{\varepsilon_o}(N_+ - N_e - N_-)$$

$$\frac{\partial N_e}{\partial t} = \alpha K_e N_e |\vec{E}| - a_e N_e - \beta N_e N_+ - \nabla \cdot (N_e K_e \vec{E})$$

$$\frac{\partial N_+}{\partial t} = \alpha K_e N_e |\vec{E}| - \beta N_e N_+ - \gamma N_- N_+ - \nabla \cdot (N_+ K_+ \vec{E})$$

$$\frac{\partial N_-}{\partial t} = a_e N_e - \gamma N_- N_+ - \nabla \cdot (N_- K_- \vec{E})$$

where

e = electron charge

N_e, N_+, N_- = electron, positive ion and negative ion densities (m^{-3})

α = Townsend's first ionization coefficient (m^{-1}), which is usually given by $\alpha = Ap \exp[-Bp/|\vec{E}|]$, p is the gas pressure and A and B are

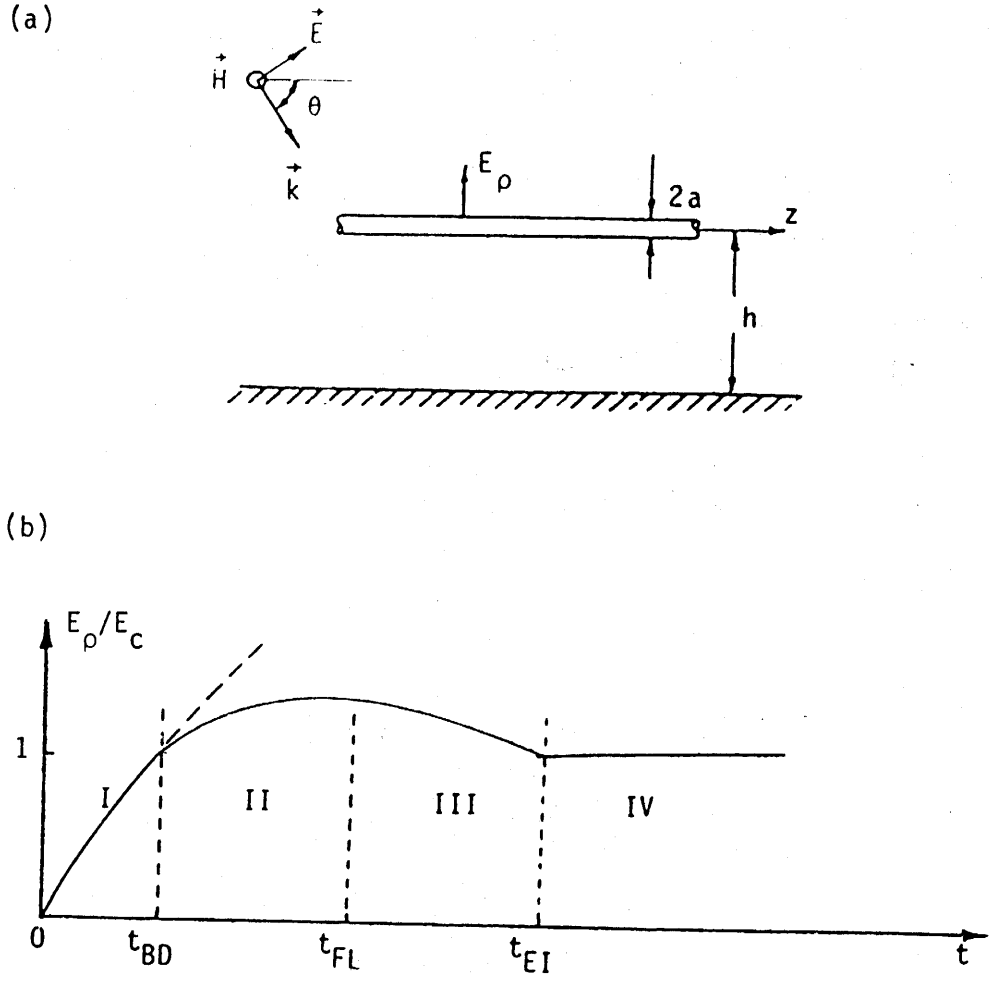

Figure 33. (a) Geometry of the problem; (b) different time domains for analyzing the effect of corona. The curve illustrates a possible time variation of induced electric field on the wire.

two parameters

a_e = electron attachment rate (sec^{-1})

β, γ = recombination rates ($m^3 sec^{-1}$)

K_e, K_+, K_- = electron, positive ion and negative ion mobilities ($m^2 volt^{-1} sec^{-1}$)

Near the surface of the wire, $\vec{E} = E_\rho \vec{e}_\rho$ and $\frac{\partial}{\partial \phi} = 0$. The above equations can be simplified as follows:

$$\frac{\partial^2 E_\rho}{\partial z^2} - \mu_o \varepsilon_o \frac{\partial^2 E_\rho}{\partial t^2} = \mu_o \frac{\partial}{\partial t}[(K_e N_e + K_+ N_+ + K_- N_-) e E_\rho]$$

$$\frac{1}{\rho} \frac{\partial}{\partial_\rho} (\rho E_\rho) = \frac{e}{\varepsilon_o} (N_+ - N_e - N_-)$$

$$\frac{\partial}{\partial z} (N_+ - N_e - N_-) = 0$$

$$\frac{\partial N_e}{\partial t} = \alpha K_e N_e |E_\rho| - a_e N_e - \beta N_e N_+ - \frac{1}{\rho} \frac{\partial}{\partial \rho} (\rho N_e K_e E_\rho)$$

$$\frac{\partial N_+}{\partial t} = \alpha K_e N_e |E_\rho| - \beta N_e N_+ - \gamma N_- N_+ - \frac{1}{\rho} \frac{\partial}{\partial \rho} (\rho N_+ K_+ E_\rho)$$

$$\frac{\partial N_-}{\partial t} = a_e N_e - \gamma N_- N_+ - \frac{1}{\rho} \frac{\partial}{\partial \rho} (\rho N_- K_- E_\rho)$$

Various approximations to the above equations can be made in different time domains which are shown in Figure 33b. The domains are defined as follows:

I. Linear domain:

The time interval extends from $t = 0$ to $t = t_{BD}$ (a few tens of ns), t_{BD} being the time for air breakdown when $E_\rho = E_c$. In this domain, the air surrounding the wire behaves as free-space, i.e. N_e, N_+, $N_- = 0$. The

linear HEMP effect on the wire is presented in the text.

II. Avalanche domain:

In this domain, the radial electric field is strong enough to ionize the air and the avalanche process is the dominant mechanism, meaning that a_e, β, γ terms are negligible in the equations. This time interval lasts until the time t_{FL} (the so-called Formative Lag time) when the avalanche process creates a space charge field of a magnitude comparable to the applied field ($E_{\text{space charge}} \simeq E_{\text{applied}}$).

III. Electron-Ion transition domain:

In this domain, electron attachment rate is comparable to the avalanche rate. As a result, electrons attach to neutral atoms and create negative ions. Recombination can still be ignored, i.e., β, γ terms are negligible in the equations. The time interval lasts until $t = t_{EI}$ which is determined by $N_-/N_e \simeq 100$.

IV. Quasi-static domain:

In this domain which is dominated by recombination, the corona is fully established, and the radial component of the electric field on the surface of the wire becomes E_c. The non-linear transmission line is one of the models that may be used in this domain.

As can be seen, different time domains must be considered in order to investigate the effect of corona on responses of transmission and distribution lines to HEMP. In each domain the corona equations will be simplified according to conditions appropriate for that domain. Different boundary and initial conditions will apply in each domain. The corona equation together with the boundary and initial conditions should then be studied, both analytically and numerically, in each domain, and the theoretical results should be compared with available experimental data.

OAK RIDGE NATIONAL LABORATORY
OPERATED BY MARTIN MARIETTA ENERGY SYSTEMS, INC.

POST OFFICE BOX X
OAK RIDGE, TENNESSEE 37831

July 16, 1985

C. E. Baum
NTYEE
Kirkland AFB, NM 87117

Dear Carl:

All papers and notes submitted to AFWL for publication in the AFWL EMP Note Series are cleared for public release. We have clearance documentation on IN 441, IN 436, and TN 351. The documentation for IN 435 has been misfiled and we are attending to that problem.

Once again, all notes and papers that we submit to your office are cleared. A few notes by LuTech, Inc. will not be submitted to AFWL because of classification. If you have any further questions, please let me know.

Sincerely,

Kindy Barnes

P. R. Barnes

PRB/mm